DMD Fast Forward. Published on March 14, 2007 as DOI: 10.1124/dmd.106.014266
DMD Fast Forward. Published on March 14, 2007 as doi:10.1124/dmd.106.014266
This article has not been copyedited and formatted. The final version may differ from this version.

"DMD#14266"

METABOLISM, PHARMACOKINETICS, AND EXCRETION OF THE SUBSTANCE P RECEPTOR ANTAGONIST CP-122,721 IN HUMANS: STRUCTURAL CHARACTERIZATION OF THE NOVEL MAJOR CIRCULATING METABOLITE 5-TRIFLUOROMETHOXY SALICYLIC ACID (TFMSA) BY HPLC/MS/MS AND NMR SPECTROSCOPY

KEVIN COLIZZA, MOHAMED AWAD AND AMIN KAMEL

Pfizer Global Research and Development, Groton, CT 06340

Downloaded from dmd.aspetjournals.org at ASPET Journals on June 24, 2024

Copyright 2007 by the American Society for Pharmacology and Experimental Therapeutics.

DMD Fast Forward. Published on March 14, 2007 as DOI: 10.1124/dmd.106.014266
This article has not been copyedited and formatted. The final version may differ from this version.

"DMD#14266"

Running Title:

Metabolism and Disposition of CP-122,721 in humans

Address for Correspondence: Amin Kamel, Ph. D., Exploratory Medicinal Sciences, Pfizer Global Research and Development, Groton Laboratories, Groton, CT 06340, Tel: 860-441-1848, Fax: 860-715-7588, E-mail. Amin.m.kamel@pfizer.com

Text pages 26

Tables 4

Figures 16

References 13

Abstract 259

Introduction 235

Discussion 1,063

[1]Abbreviations used are: CP-122721-01 (+)-2S,3S)-3-(2-methoxy-5-trifluoromethoxybenzlamino)-2-phenylpiperidine hydrochloride hydrate); SP, substance P; NK_1, neurokinin-1; HPLC, high pressure liquid chromatography; radio-HPLC, HPLC with on-line radioactivity detection; β-RAM, radioactivity monitor; LC-ARC, liquid chromatography-accurate radioactivity counting; C_{max}, peak plasma concentration; T_{max}, time at which C_{max} occurred; AUC, area under the plasma concentration-time curves; CID, collision induced dissociation; SIM, Selected ion monitoring; MRM, multiple reaction monitoring; RAD, radioactivity detector.

Downloaded from dmd.aspetjournals.org at ASPET Journals on June 24, 2024

DMD Fast Forward. Published on March 14, 2007 as DOI: 10.1124/dmd.106.014266
This article has not been copyedited and formatted. The final version may differ from this version.

ABSTRACT:

The metabolism, pharmacokinetics and excretion of a potent and selective substance P receptor antagonist CP-122,721 have been studied in six healthy male human subjects (4 extensive metabolizers (EM) and 2 poor metabolizers (PM) of CYP2D6) following oral administration of a single 30 mg dose of ^{14}C-CP-122,721. Approximately 84% of the administered radioactivity was recovered from the urine and feces of the subjects over a period of 312 hours. Approximately 80% of the dose for EM subjects was recovered within 48 hours. PM Subjects, however, excreted only about 45% of the dose in 48 hours and required the full 312 hours to achieve nearly 80% recovery. Absorption of CP-122,721 was rapid in both extensive and poor metabolizers, as indicated by the rapid appearance of radioactivity in serum. The serum concentrations of total radioactivity were always much greater than unchanged drug indicating early formation of metabolites. The average CP-122,721 $t_{1/2}$ was 6.7 and 45.0 h for EM and PM subjects, respectively. The serum concentrations of CP-122,721 reached a peak of 7.4 and 69.8 ng/ml for extensive and poor metabolizers, respectively. The major metabolic pathways of CP-122,721 were due to O-demethylation, aromatic hydroxylation, and indirect glucuronidation. The minor metabolic pathways included: aliphatic oxidation at the piperidine moiety, O-dealkylation of the trifluoromethoxy group, N-dealkylation and oxidative deamination. In addition to the major human circulating metabolite 5-trifluoromethoxy salicylic (TFMSA), all other circulating metabolites of CP-122,721 were glucuronide conjugates of oxidized metabolites. TFMSA was identified using HPLC/MS/MS and NMR and mechanisms were proposed for its formation. There are no known circulating active metabolites of CP-122,721.

Downloaded from dmd.aspetjournals.org at ASPET Journals on June 24, 2024

DMD Fast Forward. Published on March 14, 2007 as DOI: 10.1124/dmd.106.014266
This article has not been copyedited and formatted. The final version may differ from this version.

Introduction

CP-122,721, (+)-(2S,3S)-3-(2-methoxy-5-trifluoromethoxybenzylamino)-2-phenylpiperidine, is a potent, selective and orally active substance P (SP) receptor antagonist that is expected to be therapeutically efficacious in treating diseases characterized by excessive SP receptor stimulation. SP is a mammalian tachykinin that is widespread in both the central and peripheral nervous systems. CP-122,721 causes antagonism through its action on the neurokinin-1 (NK1) receptor (one of three NK receptor subtypes), to which SP binds. Available evidence suggests that SP antagonists have therapeutic value in depression, schizophrenia, pain, and inflammation. New information suggests a role for SP in Major Depressive Disorder (MDD). In addition, SP antagonists may be beneficial in the relief of anxiety (Herpfer et al., 2005; Nakayama et al., 2004; Duffy et al., 2002)

Metabolism and pharmacokinetic studies in rat (Kamel et al., 2006) indicated that CP-122,721 is extensively metabolized resulting in low drug concentrations in the systemic circulation. Most of the metabolic pathways of CP-122,721 were similar in both rats and humans. However, one additional route of metabolism was detected only in humans (not in rats) and this led to the formation of the major circulating metabolite 5-trifluoromethoxy salicylic acid (TFMSA). The metabolism of CP-122,721 was investigated in beagle dogs; another toxicology species used for safety studies, and routes of metabolism were determined. The formation of TFMSA metabolite was detected in dog plasma at considerably lower levels compared to humans and results may suggest that dog is the most relevant preclinical species in which metabolism of CP-122,721 could be studied for extrapolating results to humans (Kamel A, Du Y, Colizza K and

Downloaded from dmd.aspetjournals.org at ASPET Journals on June 24, 2024

DMD Fast Forward. Published on March 14, 2007 as DOI: 10.1124/dmd.106.014266
This article has not been copyedited and formatted. The final version may differ from this version.

Prakash C, unpublished results). There are no known circulating active metabolites of CP-122,721 including TFMSA.

The objective of the present study was to investigate the metabolism, excretion and pharmacokinetics of CP-122,721 in humans. The metabolites of CP-122,721 were tentatively identified by ion spray LC/MS/MS using collision induced dissociation (CID), neutral loss (NL), total ion current (TIC), and precursor ion scanning techniques. NMR spectroscopy was also utilized to identify the major human circulating metabolite 5-trifluoromethoxy salicylic acid (TFMSA).

Downloaded from dmd.aspetjournals.org at ASPET Journals on June 24, 2024

Material and Methods

General Chemicals. Commercially obtained chemicals and solvents were of HPLC or analytical grade. Luna HPLC columns were obtained from Phenomenex (Torrance, CA). Ecolite (+) scintillation cocktail was obtained from ICN (Irvine, CA). β-glucuronidase from Helix Pomatia (type H-1 with sulfatase activity) was obtained from Sigma Chemical Company (St. Louis, MO). Human liver S9 fraction was purchased from BD-Gentest (Woburn, MA).

Radiolabelled Drug and Reference Compounds. [^{14}C]CP-122,721 (HCl salt, Fig. 1), labeled at the benzylic position of the trifluoromethoxy anisole moiety was synthesized by the radiochemistry group at Pfizer Global Research and Development (Groton, CT). [^{14}C]CP-122,721 has a specific activity of 1.27 mCi/mmol and a radiochemical purity of ≥99 % as determined by radio-HPLC. CP-114,621 [(2S,3S)-2-phenyl-piperidin-3-ylamine], CP-125,611 [(2-[((2S,3S)-2-phenyl-piperidin-3-ylamino)-methyl]-4-trifluoromethoxy-phenol] and CP-677,623 [2-methoxy-5-trifluoromethoxy-benzylamine] were synthesized by the Medicinal Chemistry group at Pfizer Global

DMD Fast Forward. Published on March 14, 2007 as DOI: 10.1124/dmd.106.014266
This article has not been copyedited and formatted. The final version may differ from this version.

Research and Development (Groton, CT) and served as synthetic standards to confirm the structures of metabolic pathways intermediates, where applicable.

Urinary and Fecal Excretion Study. Mass balance and excretion study was conducted in six healthy male human subjects (4 extensive metabolizers (EM) of CYP2D6, subjects 1-4, and 2 poor metabolizers (PM) of CYP2D6, subjects 5-6). Human subjects were administered a single 30 mg (free base) oral dose of CP-122,721 containing 100 μCi of ^{14}C-CP-122,721. Urine and feces were collected from the subjects in 24-hour intervals for a minimum of 7 days to a maximum of 13 days post dose. The first urine sample was collected at 0-12 hours post dose. All biological samples were stored at -20 ^{o}C until analysis. Sample analysis was carried out within days after the completion date of the study and metabolite profiles were obtained on pooled samples.

Pooling Methods to Obtain Quantitative and Qualitative Data.

It is essential that quantitative metabolite profiling represent accurate metabolite percentages relevant to AUC (or C_{avg}) rather than an arbitrary plasma pool.

For quantitative profiling of metabolites in excreta (urine, feces), samples were pooled from each individual in proportion to the amount (weight or volume) of excreta in each sampling period. For subsequent metabolite identification (qualitative analysis), the most concentrated samples were used to avoid unnecessary dilution of metabolites.

For quantitative profiling of metabolites in circulation, pooling was done according to the method whereby samples are pooled in proportion to the time interval each sample represents (Hamilton et al.,1981; Riad et al., 1991; Hop et al., 1998). Serum samples were pooled such that at least 80% of total radiolabel AUC is captured. For

Downloaded from dmd.aspetjournals.org at ASPET Journals on June 24, 2024

DMD Fast Forward. Published on March 14, 2007 as DOI: 10.1124/dmd.106.014266
This article has not been copyedited and formatted. The final version may differ from this version.

subsequent metabolite identification, the most concentrated samples were utilized to avoid dilution of circulating drug-related materials

Analysis of Serum Metabolites. For serum profiles and metabolites identification, blood samples were collected into non-heparinized vacutainers at the following time points: 1, 4, 8, 12, and 24 hours post dose. The blood samples were centrifuged at 4^{o}C and serum was transferred to clean tubes. Serum samples were pooled as described above by human subject and stored at -20 ^{o}C until analysis.

Determination of Radioactivity. Quantification of total radioactivity in urine and serum was determined by counting sample aliquots (50-100 µl) using a ^{14}C program on either a Beckman Model LS 3801 or LS 5000TD liquid scintillation counter (Ontario, Canada). Ecolite (+) scintillation cocktail (5 ml, ICN, Irvine, CA) was used for determination of the radioactivity in the samples. Quench curves were prepared separately for [^{14}C]CP-122,721.

Fecal samples were homogenized with 50:50 ethanol:water and the total weights of the fecal homogenate were recorded. Aliquots (100-300 mg, in triplicate) of the homogenates were air-dried and combusted in a Harvey OX-300 or OX-500 biological sample oxidizer (R. J. Harvey Instrument Corporation; Hillsdale, NJ). The liberated $^{14}CO_2$ was trapped in scintillation Carbon-14 Cocktail (15 ml, R. J. Harvey Instrument Corporation) and the radioactivity in the trapped samples was determined by counting in a liquid scintillation counter. Combustion efficiencies were determined by combusting [^{14}C] standards (Spec-Chec, Perkin Elmer Life Sciences, Wellesley, MA) in an identical manner. The samples obtained at pre-dose were used as controls and counted to obtain a background count rate. The amount of radioactivity in the dose was expressed as 100 %

Downloaded from dmd.aspetjournals.org at ASPET Journals on June 24, 2024

DMD Fast Forward. Published on March 14, 2007 as DOI: 10.1124/dmd.106.014266
This article has not been copyedited and formatted. The final version may differ from this version.

and the radioactivity in urine and feces at each sampling time was expressed as the percentage of dose excreted in the respective matrices at that sampling time.

Concentrations of Total Radioactivity and CP-122,721

Blood samples (10 mL) from each subject (N=6) were collected into non-heparinized vacutainers at the following time points: 0.5, 1, 2, 3, 4, 6, 8, 12, 24, 36, 48, 72, 96, 144, 196 and 240 hours post dose and were centrifuged. The resulting serum samples were placed into clean tubes for shipment and subsequent analysis. Total radioactivity in serum was determined by counting 50 µL aliquots from each sample in duplicate using a ^{14}C program on a Wallac #1409 liquid scintillation counter. Ecolite (+) scintillation cocktail (~7.0 mL, ICN, Costa Mesa, CA) was used for the determination of radioactivity in the samples. Total radioactivity in the serum samples were converted into ng equivalent/mL based on the dose received by each patient (30 mg CP-122,721, 100 µCi ^{14}C per patient). Serum concentrations of the unchanged CP-122,721 (ng/mL) were determined by a validated HPLC/MS/MS assay (Kamel et al., 1997).

Pharmacokinetic Analysis. Pharmacokinetic parameters were calculated using the WinNonLin software (V02.1A; Pharsight Corp., Palo Alto, CA). The areas under the CP-122,721 and total radioactivity concentration time curves (AUC) were calculated from serum concentrations of CP-122,721 and total radioactivity using a trapezoidal approximation of area, using zero as the time zero concentration. T_{max} was the time of the first occurrence of the maximal serum concentration (C_{max}). Noncompartmental model analysis was used to estimate the pharmacokinetics parameters.

Extraction of Metabolites from Biological Samples. Urine samples were pooled (0-72 h for EM subjects and 0-192 h for PM subjects) as described above. The

Downloaded from dmd.aspetjournals.org at ASPET Journals on June 24, 2024

DMD Fast Forward. Published on March 14, 2007 as DOI: 10.1124/dmd.106.014266
This article has not been copyedited and formatted. The final version may differ from this version.

pooled samples were vortex-mixed and 10 mL from each pool was evaporated to dryness in a Turbo evaporator (Zymark, Hopkinton, MA). The residue was reconstituted in 0.5 mL of 5/95 acetonitrile/water and then transferred to 1.5-mL eppendorf tubes and centrifuged at 14,000 rpm for about 2 min. Aliquots (10 µl) of the supernatants were directly injected without further purification onto the LC-ARC system which stopped the flow every 10 seconds and counted for 60 seconds. The LC system is described below.

A fraction of the total fecal sample mass from each human time point was pooled from 0-96, 0-48, 0-120, 72-168, 24-120 and 12-168 hours for subjects 1, 2, 3, 4, 5 and 6, respectively. From the pooled samples (~100-200 g), aliquots (~10 g) were suspended in 25 mL of acetonitrile (ACN). Suspensions were sonicated (~20 min.), vortexed and centrifuged at approximately 3200 rpm for 6 min. Following the measured supernatant transfer to clean, 15-mL conical tubes, duplicate aliquots (100 µl) from each extraction were counted in a liquid scintillation counter. The total recovery of radioactivity averaged 94%. The supernatants were evaporated to dryness under nitrogen in a Turbo Vap LV evaporator operated at 37 °C. The residues were reconstituted in 2 mL of mobile phase. Aliquots (100 µl) of concentrated fecal extracts were injected onto the LC-ARC system. Due to the very low levels of radioactivity in the feces, highly concentrated samples were necessary to obtain radiochromatograms. This presented numerous background problems for radiochemical detection. The problem was resolved on the LC-ARC system by allowing the first 5 minutes of the analysis to be performed non-stop flow, then performing stop flow analysis from 5 to 45 minutes.

Serum samples were pooled by human subject separately from each sampling time, 1, 4, 8, 12 and 24 hour post dose and aliquots of 1.5 mL from each pool were extracted with 5 mL of acetonitrile. The mixtures were vortex mixed for 5 minutes and

Downloaded from dmd.aspetjournals.org at ASPET Journals on June 24, 2024

DMD Fast Forward. Published on March 14, 2007 as DOI: 10.1124/dmd.106.014266
This article has not been copyedited and formatted. The final version may differ from this version.

centrifuged at 3500 rpm for 5 minutes to remove the precipitated proteins. Supernatants were combined and a small aliquot of supernatant was counted. Approximately 96% (average of all subjects) of the radioactivity was recovered in the supernatant. The supernatants were evaporated under N_2 in a turbovap at room temperature. The residues were reconstituted with mobile phase and aliquots of 100 μL for each subject were injected on the HPLC system for profiling and metabolite identification.

Quantitative Assessment of Metabolite Excretion. Quantification of the metabolites was carried out by measuring radioactivity in the individual HPLC-separated peaks using a β-RAM instrument (IN/US, Tampa, FL). The β-RAM provided an integrated printout in cpm and the percentage of the radiolabelled material, as well as peak representation. The β-RAM was operated in the homogeneous liquid scintillation counting mode with addition of 4 ml/min of Ecolite scintillation cocktail to the eluent after-UV detection. Urinary, fecal and serum profiles were quantitatively very similar over time for at least 12 months indicating sample stability in these matrices.

Enzyme Hydrolysis. Pooled human urine samples (~ 10 mL) were adjusted to pH 5 with sodium acetate buffer (0.1 M) and treated with 2,500 units of β-glucuronidase/sulfatase. The mixture was incubated in a shaking water bath at 37 ^{o}C for 12 h and was diluted with acetonitrile (~10 mL). The precipitated protein was removed by centrifugation. The pellet was washed with an additional 2 ml of acetonitrile and both supernatants were combined. The supernatant was concentrated, dissolved in 0.5 ml of mobile phase and an aliquot (50 μl) was injected on the HPLC. Incubation of the urine samples without the enzyme served as a control.

Formation, HPLC Isolation and Purification of 5-trifluoromethoxy salicylic acid (TFMSA) Metabolite from [^{14}C]-CP-122,721 Incubation with Human Liver S9 Fraction

Downloaded from dmd.aspetjournals.org at ASPET Journals on June 24, 2024

DMD Fast Forward. Published on March 14, 2007 as DOI: 10.1124/dmd.106.014266
This article has not been copyedited and formatted. The final version may differ from this version.

[^{14}C]CP-122,721 (27 μM) was incubated with human liver S9 fraction (HL-1123; 37 mg/mL protein) in the presence of 100 mM potassium phosphate buffer, pH 7.4, and cofactor solution (9 mM $MgCl_2$, 0.54 mM NADP, 6.2 mM DL-isocitric acid, and 0.5 U/mL isocitric dehydrogenase) in a total volume of 10 mL. The reaction mixture was initiated by the addition of the S9 fraction (~ 1.35 mL, total of ~ 50 mg protein) and incubation was carried out in a shaking water bath at 37^{o}C. The reaction mixture was incubated for 16 hr and stopped by the addition of acetonitrile (5 mL). The mixture was vortex mixed for 5 min and centrifuged at 3500 rpm for 5 min to remove the precipitated proteins. The supernatant was evaporated under N_2 in a turbovap at room temperature. The residue was reconstituted with mobile phase and aliquots of 100 μL were injected onto the HPLC system for purificationg. The 5-trifluoromethoxy salicylic acid metabolite was isolated and purified using HPLC system described below. The purified HPLC fraction (27-30 min) was dried under N_2 stream and stored at –20^{o}C until use.

Chemical synthesis of 5-trifluoromethoxy salicylic acid

A novel metabolite was synthesized chemically by carboxylation and demethylation of 2-Bromo-1-methoxy-4-trifluoromethoxy-benzene to serve as a standard for HPLC, NMR and mass spectral studies (Fig. 2).

Synthesis of 2-Methoxy-5-trifluoromethoxy-benzoic acid

To the solution of 2-bromo-1-methoxy-4-trifluoromethoxy-benzene (1.0 g, 3.69 mmol) in anhydrous ether (50 mL), at –78 ^{o}C, under a nitrogen atmosphere, was added n-butyl lithium, n-BuLi, (0.738 mL, 1.85 mmol, 2.5M solution in hexane) over 5 minutes, while magnetically stirring. After 15 minutes, anhydrous carbon dioxide was bubbled through the reaction mixture for 10 minutes. It was allowed to warm up to room temperature.

Downloaded from dmd.aspetjournals.org at ASPET Journals on June 24, 2024

DMD Fast Forward. Published on March 14, 2007 as DOI: 10.1124/dmd.106.014266
This article has not been copyedited and formatted. The final version may differ from this version.

The ethereal solution was washed with a 5% solution of aqueous sodium hydroxide (3 X 50 mL). The combined aqueous solution was acidified with 1N solution of hydrochloric acid (pH 2) then extracted with ether (3 x 200mL). The combined ethereal solution was dried over anhydrous sodium sulfate and concentrated to give ~ 0.26 g of an off white solid. No further purification was attempted. A sample of the off white solid product, approximately 15 mg, was taken for structure confirmation by NMR as described below.

Synthesis of 5-trifluoromethoxy salicylic acid (TFMSA)

To a solution of the off white solid product 2-methoxy-5-trifluoromethoxy-benzoic acid (23.6 mg, 0.1 mmol) in anhydrous methylene chloride (0.9 mL) was added, boron tribromide (0.100 mL, 1M solution in methylene chloride) at 0 ^{o}C. The reaction was allowed to continue for 16 hours. The solution was made acidic (pH 0) using 1N solution of hydrochloric acid, and extracted with ethyl acetate (3 x 3 ml). The ethyl acetate solution was dried over anhydrous sodium sulfate, filtered and concentrated to give ~ 11 mg of a white solid. No further purification was attempted. The structure identification of the white solid was accomplished using mass spectral analysis and standard NMR proton-proton experiments. Complete ^{1}H chemical shifts were obtained and reported in ppm. The white solid was used for NMR and MS analyses as described below.

LC/MS/MS. LC/MS/MS was conducted with a SCIEX API III^{plus} (Perkin-Elmer, Thornhill, Ontario, Canada) equipped with an ionspray source. The effluent from the HPLC column was split and about 50 µl/min was introduced into the atmospheric pressure ionization source. The remaining effluent was directed into the flow cell of the β-RAM. The β-RAM response was recorded in real time by the mass spectrometer data system that provided simultaneous detection of radioactivity and mass spectrometry data. The delay in response between the two detectors was about 0.2 min with the mass

Downloaded from dmd.aspetjournals.org at ASPET Journals on June 24, 2024

DMD Fast Forward. Published on March 14, 2007 as DOI: 10.1124/dmd.106.014266
This article has not been copyedited and formatted. The final version may differ from this version.

spectrometric response recorded earlier. The ionspray interface was operated at 6000 V and the mass spectrometer was operated in the positive mode. Collision induced dissociation (CID) studies were performed using argon gas at a collision energy of 25-28 eV and a collision gas thickness of 3.5 x 10^{14} molecules/cm^2.

HPLC. The HPLC system consisted of a Rheodyne injector for manual injections, a LDC/Milton Roy constametric CM4000 gradient pump, a Waters Lambda-Max model 481 UV detector, a radioactive monitor (β-RAM; IN/US, Tampa, FL) and a SP 4200 computing integrator. Chromatography was carried out on a Phenomenex Luna HPLC column [4.6 x 150 mm, 5 μm d_p, C-18(2)] with a binary mixture of acetonitrile (solvent A) and 10 mM ammonium acetate (pH 5.0 with acetic acid, solvent B). A flow rate of 1.0 ml/min was used for all analyses. The mobile phase initially consisted of solvent A/solvent B (5/95) for a 10-min period. It was then linearly programmed to achieve a mixture of solvent A/solvent B (40/60) over a 20-minute period and operated isocratically for 5 min under these conditions. The mobile phase was then linearly programmed to achieve a mixture of solvent A/solvent B (80/20) over a 5-min period and operated isocratically for 5 min under these conditions. It was then linearly programmed to return to the initial mixture of solvent A/solvent B (5/95) over a 5-min period. This gave a total run time of 50 min with an additional time of 10 min for column re-equilibration between injections. The retention times of radioactive peaks were compared with the synthetic standards.

Liquid Chromatography-Accurate Radioisotope Counting (LC-ARC)

The LC-ARC system maintained the same chromatography conditions as above and was equipped with advanced stop flow controller and ARC data system (AIM

Downloaded from dmd.aspetjournals.org at ASPET Journals on June 24, 2024

DMD Fast Forward. Published on March 14, 2007 as DOI: 10.1124/dmd.106.014266
This article has not been copyedited and formatted. The final version may differ from this version.

Research Co., Newark, DE). The flow cell (2.2 mL volume) and cocktail were obtained from AIM Research Co. The flow was stopped in 10-second intervals and counted for 60 seconds. The 10 seconds of flow (~0.17 mL) mixes with enough Tru-count scintillation cocktail to fill the cell for any given stop-flow period. The background counting threshold is 30 CPM.

LC-ARC provides several advantages over traditional detection systems. The typical limit of detection of LC-ARC is 5-20 DPM for ^{14}C and 10-40 DPM for ^{3}H. The sensitivity is 10-20 fold better than that of traditional flow-through detection systems. The LC-ARC method dramatically improves the radioactivity counting accuracy and reduces the radioactive wastes. LC-ARC eliminates the need of collecting fractions for off-line counting for low level radioactivity thus reducing the study cost (Nassar et el., 2003; Wang et al., 2005)

Nuclear Magnetic Resonance

Nuclear magnetic resonance experiments were performed at 400 MHz (^{1}H) on a Varian-400 spectrometer. The temperature was set to 298K throughout the analysis and samples were dissolved in DMSO-d_6. Typical 1D proton experiments were performed over the spectral range 0-8 or 0-13 parts per million (ppm).

Results

Excretion. As shown in Table 1, after a single oral dose of ^{14}C-CP-122,721 to humans, the majority of the radioactivity was excreted in the urine. At 312 hours after the dose, the percent of radioactivity excreted in urine averaged 80.7±4.9% and 71.1% in EM and PM, respectively. The corresponding percent of radioactivity excreted in feces averaged 6.6±3.6% and 6.9% in EM and PM, respectively. Nearly 80% of the excreted

Downloaded from dmd.aspetjournals.org at ASPET Journals on June 24, 2024

DMD Fast Forward. Published on March 14, 2007 as DOI: 10.1124/dmd.106.014266
This article has not been copyedited and formatted. The final version may differ from this version.

radioactivity recovery occurred in the first 48 hours for EM subjects while only about 50% was recovered for PM subject in the same time interval (Fig. 3).

Pharmacokinetics. The mean serum concentration-time curves for CP-122,721 (ng/ml) and total radioactivity (ng-equivalent/ml) for EM and PM human subjects are shown in Figure 4. Absorption of CP-122,721 was rapid in both EM and PM subjects, as indicated by the rapid appearance of radioactivity in serum after the oral administration of [^{14}C]CP-122,721. The serum concentrations of total radioactivity were always much greater than unchanged drug, indicating early formation of metabolites. As shown in Table 2, the terminal phase $t_{1/2}$ in EM and PM subjects were approximately 4 and 1.2 times higher, respectively, for total radioactivity than for unchanged CP-122,721 (CP-122,721 $t_{1/2}$ was 6.7 and 45 h for EM and PM, respectively. The total radioactivity $t_{1/2}$ was 23.7 and 55.2 h for EM and PM, respectively. The serum concentrations of CP-122,721 reached a peak of 7.4 and 69.8 ng/ml for EM and PM, respectively. The serum concentrations of total radioactivity reached a peak of 844 and 447 ng equivalent/ml for EM and PM, respectively. Based on AUC(0-tlast), 0.5% and 16% of the circulating radioactivity was attributable to unchanged drug for EM and PM subjects, respectively, and the balance, approximately 99.5 and 84 % of the serum radioactivity was due to metabolites.

Metabolic Profiles in Biological Samples

Urine. Representative HPLC radiochromatograms of metabolites in urine from EM (subject 2, 0-72 hr post dose pooled) and PM (subject 6, 0-192 hr post dose pooled) following oral administration of [^{14}C]-CP-122,721 with on-line radioactivity monitoring are depicted in Figure 5. A total of eleven metabolites in EM subject and eight

Downloaded from dmd.aspetjournals.org at ASPET Journals on June 24, 2024

DMD Fast Forward. Published on March 14, 2007 as DOI: 10.1124/dmd.106.014266
This article has not been copyedited and formatted. The final version may differ from this version.

metabolites in PM subjects were identified. M4 was the major metabolite in EM subject and the major metabolite in PM subjects, however, was M19.

Feces. Representative LC-ARC profiles of metabolites in fecal samples from EM (subject 1, 0-96 hr post dose pooled) and PM (subject 5, 24-120 hr post dose pooled) are shown in Figure 6. CP-122,721 and 3 metabolites were detected in the chromatograms. The percentages of metabolites excreted in both urine and feces in relation to dose for EM and PM subjects as well as their description are presented in Table 3.

***Serum*.** Representative profiles of serum metabolites from EM and PM subjects (1, 4, 8 ,12, and 24 hr pooled) are depicted in Figure 7. The average percentages of each metabolite recovered in serum of EM and PM male human subjects following oral administration of [^{14}C]-CP-122,721 are shown in Table 4. Qualitative and quantitative similarities were observed for all EM subjects. Similarly, qualitative and quantitative similarities were also observed for the two PM subjects. However, there are quantitative and some qualitative differences between EM and PM subjects. Unchanged drug was only detected in the radiochromatogram of one PM human subject. CP-122,721 and a total of 4 metabolites accounted for approximately 99 % (average of EM and PM subjects) of the total radioactivity.

Identification of Metabolites

The structures of metabolites were elucidated by ionspray LC/MS/MS using both positive and negative ion modes. Combined liquid chromatography/ionspray mass spectrometry (full scan) and tandem mass spectrometry, such as precursor ion, product ion, single ion monitoring (SIM) and multiple reaction monitoring (MRM) scanning techniques were used for the identification of metabolites. Where possible, the identities of metabolites

Downloaded from dmd.aspetjournals.org at ASPET Journals on June 24, 2024

DMD Fast Forward. Published on March 14, 2007 as DOI: 10.1124/dmd.106.014266
This article has not been copyedited and formatted. The final version may differ from this version.

were confirmed by co-elution on HPLC with synthetic standards. The word "tentative" was utilized when the exact sites of some structural modification could not be determined.

Synthetic standard of CP-122,721 had a retention time of ~ 35.2 min on the HPLC system and showed a protonated molecular ion at m/z 381. The CID mass spectrum of CP-122,721 showed abundant fragment ions at m/z 160 and 205 which represent the phenyl piperidinyl moiety and the trifluoromethoxy anisole benzyl moiety, respectively (Fig. 8). The fragment ions at m/z 143, 132, and 117 were derived from the fragment ion at m/z 160. The fragment ion at m/z 177 represents the phenyl piperdinyl amine moiety. The fragment ion at m/z 91 represents the tropylium ion.

CP-122,721 and a total of 16 metabolites were identified. Unchanged drug was found in both urinary and fecal samples of PM subjects and was only detected in the serum of one PM human subject. The structures of eleven of these metabolites were identical to those identified previously in rat (Kamel et al., 2006): M1, M2, M3, M4, M5, M7, M8 and M9 and dog (Kamel A, Du Y, Colizza K, and Prakash C, unpublished results): M12, M14 and M15. M15 was a novel major circulating metabolite and required further structural confirmation. Five additional metabolites were identified, namely M16, M17, M18, M19 and M20.

Metabolite M15: M15 had a retention time of approximately 28.5 minutes and had a poor ionization efficiency. It was detected in all EM and PM subjects and accounted for approximately 56 and 29 % of the total radioactivity for EM and PM subjects, respectively. M15 was also detected in the urine of EM and PM subjects.

Incubation of [^{14}C]-CP-122,721 with Human liver S9 fraction resulted in the formation of a radioactive peak that had similar retention time of that of M15 from

Downloaded from dmd.aspetjournals.org at ASPET Journals on June 24, 2024

DMD Fast Forward. Published on March 14, 2007 as DOI: 10.1124/dmd.106.014266
This article has not been copyedited and formatted. The final version may differ from this version.

human subject. After further HPLC isolation and purification, spiking human serum from subject # 2 (EM) with the HPLC purified fraction (27-30 min) resulted in co-elution of M15 with the HPLC purified fraction (Fig. 9). Based on this data, the HPLC purified fraction from incubation of [^{14}C]-CP-122,721 with Human liver S9 was identified as M15 serum metabolite.

The CID mass spectrum of M15 is depicted in Figure 10 and showed a deprotonated molecular ion at m/z 221 suggesting M15 was a cleaved product with zero or an even number of nitrogen atoms. M15 was detected in the ^{14}C chromatogram indicating it contained the benzyl moiety of the parent drug and further suggested that the phenyl piperidine moiety had been removed.

The fragment ion at m/z 177, loss of 44 mass units (CO_2), from the deprotonated molecular ion indicated the presence of –COOH functionality and further suggested that the methylene group adjacent to 2-methoxy-5-trifluoromethoxy of the parent drug had been modified. The fragment ion at m/z 157 indicated the loss of HF from m/z at 177. The fragment ion at m/z 137 (2-hydroxy benzoate anion) indicated the presence of salicylic acid moiety and suggested that the methoxy group had been modified to hydroxyl group. The fragment ion at m/z 111, possibly derived from the loss of a neutral molecule of ethyne from the fragment ion at m/z 137, further suggested the presence of –COOH functionality. The prominent fragment ion at m/z 108, possibly derived from the loss of trifluoromethyl group moiety from the fragment ion at m/z 177, further suggested that the methoxy group had been modified to hydroxyl group. The fragment ion at m/z 91, possibly derived from the loss of hydroxyl group from the fragment ion at m/z 108 and/or derived from the loss of trifluoromethoxy group from the fragment ion at m/z 177, further suggested the presence of a phenol moiety. The prominent fragment ion at m/z 85 further suggested that the trifluoromethoxy group had not been modified. The

Downloaded from dmd.aspetjournals.org at ASPET Journals on June 24, 2024

DMD Fast Forward. Published on March 14, 2007 as DOI: 10.1124/dmd.106.014266
This article has not been copyedited and formatted. The final version may differ from this version.

fragment ion at m/z 69, derived from the neutral loss of quinone moiety from the fragment ion at m/z 177, indicated that the trifluoromethyl group was intact. The fragment ion at m/z 19, F^-, indicated that the trifluoromethyl group of the parent drug was intact. Based on these data, M15 was tentatively identified as 5-trifluoromethoxy salicylic acid.

The ^{1}H NMR spectra of 5-trifluoromethoxy salicylic acid (top) and an expansion of its aromatic region (bottom) are shown in Figure 11. The resonance at 3.81 ppm (s, 3H). corresponds to $–OCH_3$ (impurity from the starting material 2-Methoxy-5-trifluoromethoxy-benzoic acid). The two resonances at 2.47 ppm (m) and 1.95 ppm (s) correspond to DMSO (partially deuterated) and ETOAc, respectively. Other small resonances are due to residual solvents. The three aromatic resonances at 7.64 ppm (d, 1H, J = 2.9 Hz), 7.53-7.50 ppm (dd, 1H, J = 9.1, 2.9 Hz), and 7.05 ppm (d, 1H, J = 9.1 Hz) are consistent with a ring system containing three substitutions. The resonance at 13.03 ppm (broad s, 1 H) corresponds to –COOH. Based on the above data the final product was identified as 5-trifluoromethoxy salicylic acid. Human serum M15 was co-eluted with the synthetic standard on HPLC and its CID mass spectrum was identical to those from the synthetic standard and HPLC purified fraction from human liver S9 (Fig. 12). Based on the above data, human serum M15 was unambiguously identified as 5-trifluoromethoxy salicylic acid

Metabolite M16: Metabolite M16 had a retention time of ~ 9.1 minutes on the HPLC system and showed a protonated molecular ion at m/z 409, 28 mass units higher than unchanged drug. Accounting for ~2.4 % of the administered dose in urine, M16 was not detected in feces. The CID spectrum of M16 is depicted in Figure 13 and shows major fragment ions at m/z 205, 188 and 146. The fragment ions at m/z 205 is the same

Downloaded from dmd.aspetjournals.org at ASPET Journals on June 24, 2024

DMD Fast Forward. Published on March 14, 2007 as DOI: 10.1124/dmd.106.014266
This article has not been copyedited and formatted. The final version may differ from this version.

as that found in the CID spectrum of CP-122,721 suggesting that the methoxy trifluoromethoxy benzyl moiety is unchanged. The abundant signal at m/z 188, corresponds to the CP-122,721 fragment m/z 160 plus 28 amu. The peak at m/z 146 suggests the loss of CH_2CHO (42 amu) from the m/z 188 fragment. Based on the above data, M16 was tentatively identified as piperidine dione CP-122,721.

Metabolite M17: Metabolite M17 had a retention time of ~17.4 min on the HPLC system and accounted for ~ 3.8% of the administered dose in urine (average of EM and PM subjects), M17 was not detected in feces. M17 showed a protonated molecular ion at m/z 384, suggesting that the molecule contains an odd number of N atoms. The CID product ion spectrum of M17 showed the prominent fragment ions at m/z 208, 191 and 85 (Fig. 14). The ion at m/z 208, 176 amu lower than the molecular ion indicated that a glucuronide moiety was lost from a CP-122,721 cleaved product containing the radioisotope. The fragment at m/z 85 shows that the OCF_3 moiety was present. The loss of 17 amu (NH_3) from the fragment m/z 208 to form the m/z 191 fragment further suggested that the molecule has a primary amine functionality. Based on the above data, metabolite M17 was tentatively identified as the glucuronide conjugate of 2-aminomethyl-4-trifluoromethoxy phenol.

Metabolite M18: Metabolite M18 had a retention time of ~21.3 minutes on the HPLC system and accounted for ~ 10.2% of the administered dose in urine (average of EM and PM subjects), M18 was not detected in feces. Determination of the molecular ion was assisted by the full scan spectra in both positive and negative ion modes. Metabolite M18 showed an intense ion at m/z 402. The negative ion full scan mass spectrum showed a deprotonated molecular ion at m/z 383 suggesting that the ion at m/z

Downloaded from dmd.aspetjournals.org at ASPET Journals on June 24, 2024

DMD Fast Forward. Published on March 14, 2007 as DOI: 10.1124/dmd.106.014266
This article has not been copyedited and formatted. The final version may differ from this version.

402 represents the ammonium adduct of a metabolite with a molecular weight of 384. The molecular weight of M18 further suggested that the molecule has zero or an even number of nitrogen atoms. The CID product ion spectrum of $[M+NH_4]^+$ at m/z 402 (Fig. 15) showed the loss of NH_4^+ to give rise to the protonated molecular ion at m/z 385. The CID spectrum also showed two characteristic fragment ions at m/z 209 (loss of 176 amu from the protonated molecular ion) and 191 (loss of 194 amu from the protonated molecular ion) suggesting that M18 was a glucuronic acid conjugate of a cleaved product, which had undergone O-demethylation and oxidative deamination. A distinction between aromatic and aliphatic O-glucuronidation can be made by observing the differences in the fragment ion intensity and the pattern of loss of the glucuronyl moiety under MS/MS conditions (Fenselau et al., 1973; Abbot et al., 1992).

The relative abundance of the fragment ions at m/z 209 (very minor) and 191 (base peak) reflect the stability of each fragment ion (Fig. 14). Whereas phenolic glucuronidation will fragment easily by the loss of 176 amu and give rise to fragment ion at m/z 209, aliphatic O-glucuronidation will fragment by the loss of 194 amu and the production of a stable carbocation that is easily detected at m/z 191. The fragment ion at m/z 85 further suggested that the OCF_3 moiety was intact. Based on the above data, M18 was tentatively identified as the glucuronide conjugate of 2-hydroxymethyl-4-trifluoromethoxy phenol and the site of glucuronidation was determined to be aliphatic O-glucuronidation.

Metabolite M19: Metabolite M19 had a retention time of ~24.6 minutes on the HPLC system and accounted for ~ 6.3 and 17.2 % of the administered dose in urine for EM and PM subjects, respectively. M17 was not detected in feces and showed a protonated molecular ion at m/z 557, 176 amu higher than the unchanged drug,

Downloaded from dmd.aspetjournals.org at ASPET Journals on June 24, 2024

DMD Fast Forward. Published on March 14, 2007 as DOI: 10.1124/dmd.106.014266
This article has not been copyedited and formatted. The final version may differ from this version.

suggesting a glucuronide conjugate. Product ion spectrum of M19 showed prominent fragment ions at m/z 381, 364, 191 and 174 (data not shown). The fragments at m/z 174 and 191 (14 amu higher than the drug CID fragments of m/z 160 and 177) suggest oxidation, most likely α to the piperidine N followed by the loss of 2 hydrogen to form a lactam. The ion at m/z 381 resulted from the loss of 176 amu, a glucuronide conjugate. This suggests the formation of an O-desmethyl product followed by glucuronidation of the exposed phenolic oxygen. Based on this data, M19 was tentatively identified as the glucuronide conjugate of the O-desmethyl CP-122,721 lactam.

Metabolite M20: Metabolite M20 had a retention time of ~26.6 minutes on the HPLC system and accounted for ~ 7.3 and 2.7 % of the administered dose in urine for EM and PM subjects, respectively. M20 was not detected in feces showed a protonated molecular ion at m/z 573, 192 amu higher than the parent drug, suggesting conjugation. Product ion spectrum of M20 showed fragment ions at m/z 488, 397, 380, 207, 190 and 160 (data not shown). The ions at m/z 397 and 380 resulted from the loss of a glucuronide (-176 amu) and the subsequent loss of ammonia (-17 amu). The prominent ions at m/z 190 and 207 (30 amu higher than the drug CID fragments of m/z 160 and 177) indicate the addition of 2 oxygen atoms and subsequent loss of 2 hydrogen atoms from the phenyl piperidine moiety. The lack of any H_2O losses suggests that one oxidation occurs on the phenyl ring, while the other is an oxidation most likely α to the piperidine N followed by the loss of 2 hydrogens to form a lactam. The site of glucuronidation could not be determined from mass spectral information. Based on this data, M20 was identified as the glucuronide conjugate of 2-phenol-5-one-piperidine CP-122,721.

Downloaded from dmd.aspetjournals.org at ASPET Journals on June 24, 2024

DMD Fast Forward. Published on March 14, 2007 as DOI: 10.1124/dmd.106.014266
This article has not been copyedited and formatted. The final version may differ from this version.

Discussion

A solution of CP-122,721 labeled with ^{14}C at the benzylic position of the trifluoromethoxy anisole moiety was administered orally to six healthy male human subjects (4 extensive metabolizers (EM) of CYP2D6 and 2 poor metabolizers (PM) of CYP2D6) at a free base equivalent dose of 30 mg and 100 μCi of radioactivity.

Approximately 84% of the administered radioactivity was recovered from the urine and feces of the subjects over a period of 312 hours. Approximately 80% of the dose for EM subjects was recovered within 48 hours. PM subjects excreted only about 45% of the dose in 48 hours and required the full 312 hours to achieve nearly 80% recovery.

CP-122,721 was extensively metabolized in humans, since only a small amount of unchanged drug was detected in the excreta. The profiles of metabolites before and after treatment with β-glucuronidase were different, indicating that the elimination of the drug was due to Phase I metabolism and subsequent Phase II metabolic pathways. A total of 4 metabolites in feces, 12 metabolites in urine and 4 metabolites in serum were identified. In all subjects, total radioactivity recovered from the feces was between 2% and 10% of the dose and most of the recovery was obtained from the urine (65-85%).

Qualitative and quantitative similarities were observed for all EM subjects. Similarly, qualitative and quantitative similarities were also observed for the two PM subjects. However, there are quantitative and qualitative differences between EM and PM subjects.

For the EM subjects, the major component of drug related material in the excreta was tentatively identified as the glucuronide conjugated O-desmethyl metabolite M4 (~ 27.5 % of the administered dose). The PM subjects contained no detectable levels of M4,

Downloaded from dmd.aspetjournals.org at ASPET Journals on June 24, 2024

DMD Fast Forward. Published on March 14, 2007 as DOI: 10.1124/dmd.106.014266
This article has not been copyedited and formatted. The final version may differ from this version.

but rather the glucuronide conjugate of the O-desmethylated lactam, M19 was the major component of drug related material in the excreta (~17.2% of the administered dose).

Excretion of radioactivity in the feces of all subjects was quantitatively similar, but the metabolites were different. Most importantly, the EM subject feces did not contain CP-122,721, however, this was the major fecal component for the PM subjects.

The serum concentrations of total radioactivity were always much greater than unchanged drug, indicating early formation of metabolites. CP-122,721 $t_{1/2}$ was 6.7 and 45 h for extensive and poor metabolizers, respectively. The serum concentrations of CP-122,721 reached a peak of 7.4 and 69.8 ng/ml for extensive and poor metabolizers, respectively. Based on AUC(0-tlast), approximately 0.5% (EM) and 16% (PM) of the circulating radioactivity was attributable to unchanged drug. The balance, approximately 99.5 % (EM) and 84% (PM) of the serum radioactivity was due to metabolites. Of the total radioactivity extracted from the serum, the drug and metabolites (average of all human subjects) accounted for approximately 99 %. M3 was detected in the radiochromatograms of all EM and PM subjects and accounted for approximately 25 and 62 % of the total radioactivity for EM and PM subjects, respectively. M4 was only detected in the radiochromatograms of all EM subjects and accounted for approximately 14 % of the total radioactivity. M5 (isomeric structure of M3) was detected in the radiochromatograms of all EM subjects and one PM subject and accounted for approximately 5 and 2 % of the total radioactivity for EM and PM subjects, respectively. M15 (TFMSA) was detected in the radiochromatograms of all EM and PM subjects and accounted for approximately 56 and 29 % of the total radioactivity for EM and PM subjects, respectively. Unchanged drug was only detected in the radiochromatogram of one PM human subject and accounted for approximately 6 % of the total radioactivity. There are no known circulating active metabolites of CP-122,721.

Downloaded from dmd.aspetjournals.org at ASPET Journals on June 24, 2024

DMD Fast Forward. Published on March 14, 2007 as DOI: 10.1124/dmd.106.014266
This article has not been copyedited and formatted. The final version may differ from this version.

A proposed scheme for the biotransformation pathways of CP-122,721 in humans is shown in Figure 16. Based on the structures of these metabolites, three major and three minor routes of metabolism of CP-122,721 were identified. The major routes were due to O-demethylation, aromatic hydroxylation, and indirect glucuronidation. The minor routes included: aliphatic oxidation at the piperidine moiety, aliphatic oxidation at the benzylic position of the trifluoromethoxy anisole moiety, O-dealkylation of the trifluoromethoxy group and N-dealkylation and oxidative deamination to form TFMSA (M15) metabolite.

The formation of M15 could be derived from two different metabolic pathways: O-demethylation and direct oxidative deamination (by α-carbon hydroxylation) to yield 2-hydroxy-5-trifluoromethoxy-benzaldehyde intermediate and the phenyl-piperdine amine metabolite (CP-114,621), which has been identified in rat plasma (Kamel A and Prakash C, unpublished results). Subsequent oxidation of 2-hydroxy-5-trifluoromethoxy-benzaldehyde intermediate would result in the formation of M15 (Figure 17 a). The other metabolic pathway responsible for the formation of M15 is O-demethylation and N-dealkylation of the secondary amine, which proceeds by carbinolamine pathway (Figure 17 b), to give rise to the corresponding primary amine metabolite (CP-677,623) which was detected in rat plasma (Kamel A and Davis J, unpublished results) and is susceptible to oxidative deamination. Therefore, oxidative deamination of the primary amine metabolite (CP-677,623) and subsequent oxidation would result in the formation of M15.

Although TFMSA is a salicylic acid analogue, this metabolite does not appear to undergo glycine and/or glucuronide conjugation at detectable levels. Glycine conjugation of ortho-substituted benzoic acids was investigated and it has been reported that the

Downloaded from dmd.aspetjournals.org at ASPET Journals on June 24, 2024

DMD Fast Forward. Published on March 14, 2007 as DOI: 10.1124/dmd.106.014266
This article has not been copyedited and formatted. The final version may differ from this version.

extent of glycine conjugation of benzoic acids with the halogen group decreased in the order F > Cl > Br > I. The conjugation of 2-OH- substituent (salicylic acid) with glycine took place in only the kidney. The 2-CH_3O- substituent, however, exhibited no glycine conjugation in the liver and kidney. In addition, the size and the electronegativity of the substituent had a far greater influence over glycine conjugation. The authors also reported that it may be important that the substrates undergoing glycine conjugation contain a flat region coplanar to the carboxylate group (Fumiyo et al., 2000). From these findings, it is reasonable to assume that the lack of glycine conjugation of TFMSA could be attributed to the expected profound effect of the bulky trifluoromethoxy (-OCF_3) substituent in the meta-position.

In summary, the results of this study provide the first analysis of formation and excretion of metabolites of CP-12,721 in humans. Results were similar to those reported previously in rat (Kamel et al., 2006) and dog (Kamel A, Du Y, Colizza K and Prakash C, unpublished results). CP-122,721 is very rapidly eliminated in humans mainly by phase I oxidative metabolism and subsequent phase II metabolic pathways. We have reported a full characterization of a novel circulating metabolite, resulting from O-demethylation, oxidative deamination and subsequent oxidation. The identification of these metabolic pathways will have relevance to understanding the metabolism of other trifluoromethoxy-benzylamine piperidinyl anisole drugs.

Acknowledgments.

We would like to thank Dr. Klass Schilknegt for synthesizing radiolabelled CP-122,721.

Downloaded from dmd.aspetjournals.org at ASPET Journals on June 24, 2024

DMD Fast Forward. Published on March 14, 2007 as DOI: 10.1124/dmd.106.014266
This article has not been copyedited and formatted. The final version may differ from this version.

References

Abbott FS, Mutlib AE. (1992) Isolation and characterization of carbinolamide and phenolic glucuronide conjugates of (±)-N-methyl-N-(1-methyl-3,3-diphenylpropyl) formamide and N-formylmethamphetamine by FAB/MS, LC/MS/MS, and NMR. *Drug Metab Disp* **20(3)**, 451-60.

Duffy RA, Varty GB, Morgan CA, Lachowicz JE. (2002) Correlation of neurokinin (NK) 1 receptor occupancy in gerbil striatum with behavioral effects of NK1 antagonists. *J Pharmacol Exp Ther* **301(2),** 536-542.

Fenselau C, Billets S, Lietman PS. (1973) Mass spectral analysis of glucuronides *J Med Chem* **16(1),** 30-3.

Fumiyo K, Yumiko Y, Eriko O, Kazuo I, Miyoshi F (2000) Difference of the liver and kidney in glycine conjugation of ortho-substituted benzoic acids *Chemico-Biological Interactions* **125**, 39–50

Hamilton R A, Garnett W R, Kline B J (1981) Determination of mean valproic acid serum level by assay of a single pooled sample. *Clin Pharmacol Ther*. **29(3),** 408-13.

Herpfer I, Lieb K. (2005) Substance P receptor antagonists in psychiatry: rationale for development and therapeutic potential. *CNS Drugs* **19(4),** 275-293.

Downloaded from dmd.aspetjournals.org at ASPET Journals on June 24, 2024

DMD Fast Forward. Published on March 14, 2007 as DOI: 10.1124/dmd.106.014266
This article has not been copyedited and formatted. The final version may differ from this version.

Hop, CECA, Wang Z, Chen Q, Kwei G. (1998) Plasma-Pooling Methods To Increase Throughput for in Vivo Pharmacokinetic Screening. *J Pharm Sci* **87(7)**, 901-903.

Kamel A, Davis A, Potchoiba MJ and Prakash C (2006) Metabolism, pharmacokinetics and excretion of a potent tachykinin NK1 receptor antagonist (CP-122,721) in rat: Characterization of a novel oxidative pathway. *Xenobiotica*, **36(2–3),** 235–258.

Kamel A, Prakash C (1997) Determination of the substance P receptor antagonist CP-122,721 in plasma by narrow-bore high-performance liquid chromatography-ionspray tandem mass spectrometry *J Chromatogr Biomed Appl* **700(1 + 2),** 139-146.

Nakayama H, Yamakuni H, Nakayama A, Maeda Y, Imazumi K, Matsuo M, Mutoh S. (2004) Diphenidol has no actual broad antiemetic activity in dogs and ferrets. *J Pharmacol Sci* (Tokyo, Japan) **96(3),** 301-306.

Nassar AEF, Bjorge SM, Lee, DY (2003). On-Line Liquid Chromatography-Accurate Radioisotope Counting Coupled with a Radioactivity Detector and Mass Spectrometer for Metabolite Identification in Drug Discovery and Development. *Anal Chem*. **75(4),** 785-790.

Riad LE, Chan KK, Sawchuk RJ (1991) Determination of the relative formation and elimination clearance of two major carbamazepine metabolites in humans: a comparison between traditional and pooled sample analysis. *Pharm Res* **8(4),** 541-3

Downloaded from dmd.aspetjournals.org at ASPET Journals on June 24, 2024

DMD Fast Forward. Published on March 14, 2007 as DOI: 10.1124/dmd.106.014266
This article has not been copyedited and formatted. The final version may differ from this version.

Wang N, Szostek B, Folsom PW, Sulecki LM, Capka V, Buck RC, Berti WR, Gannon JT. (2005) Aerobic Biotransformation of 14C-Labeled 8-2 Telomer B Alcohol by Activated Sludge from a Domestic Sewage Treatment Plant. *Env Sci Tech* **39(2),** 531-538.

Downloaded from dmd.aspetjournals.org at ASPET Journals on June 24, 2024

DMD Fast Forward. Published on March 14, 2007 as DOI: 10.1124/dmd.106.014266
This article has not been copyedited and formatted. The final version may differ from this version.

Footnotes:

This work was presented in part at the 52nd ASMS Conference on Mass Spectrometry and allied topics, Nashville, TN 2004

Downloaded from dmd.aspetjournals.org at ASPET Journals on June 24, 2024

DMD Fast Forward. Published on March 14, 2007 as DOI: 10.1124/dmd.106.014266
This article has not been copyedited and formatted. The final version may differ from this version.

Figure Legends

Figure 1. Structure of ^{14}C-labeled CP-122,721

Figure 2. Chemical synthesis of 5-trifluoromethoxy salicylic acid by carboxylation and demethylation of 2-Bromo-1-methoxy-4 trifluoromethoxy-benzene

Figure 3. Mean Cumulative Recovery of 14C in EM and PM Humans Urine, Feces, and Total Recovery of Radioactivity (0-312 hr post dose) Following Oral Administration of 30 mg (free base)/kg of CP-122,721 (EM= extensive metabolizer, PM = poor metabolizer, urine ♦, Feces ■, total ▲)

Figure 4. Mean Serum Concentration of Total Radioactivity and Unchanged CP-122,721 in EM and PM Humans (0-240 hr post dose) After Oral Administration of 30 mg/kg of [14C]CP-122,721 (EM= extensive metabolizer, PM = poor metabolizer, drug (ng/mL) ♦, total radioactivity (ng(eq)/mL ■)

Figure 5. Representative HPLC-Radiochromatograms of Urinary Metabolites of CP-122,721 From EM (subject 2, 0-72 hr post dose pooled) and PM (subject 6, 0-192 hr post dose pooled) Humans Following Oral Administration of CP-122,721 (EM= extensive metabolizer, PM = poor metabolizer, TFMSA = trifluoromethoxy salicylic acid).

Figure 6. Representative LC-ARC Radiochromatograms of Fecal Metabolites of CP-122,721 From EM (0-96 hr post dose pooled) and PM (24-120 hr post dose pooled) Humans Following Oral Administration of CP-122,721 (EM= extensive metabolizer, PM = poor metabolizer, LC-ARC = liquid Chromatography-Accurate Radioisotope Counting))

Figure 7. HPLC-Radiochromatograms of Serum Metabolites of CP-122,721 From:
(a) Human Subject 1 (EM) and (b) Human Subject 6 (PM). Profiles represent 1, 4, 8, 12, and 24 hr pooled serum samples (EM= extensive metabolizer, PM = poor metabolizer)

Figure 8. CID Product Ion Spectrum of m/z 381 for CP-122,721 Standard

Figure 9. HPLC-Radiochromatograms of: (a) Serum Metabolites (1, 4, 8, 12, and 24 hr) of CP-122,721 (Human Subject #2, EM) (b) HPLC purified fraction from human liver S9 incubation with 14CP-122,721 (c) Human serum subject #2 (EM) spiked with HPLC purified fraction

Figure 10. Collision induced dissociation (CID) mass spectrum of M15 at m/z 221 from human serum subject #2 (1, 4, 8, 12, 24 HPD)

Figure 11. ^{1}H NMR spectra of 5-trifluoromethoxy salicylic acid (top) and an expansion of its aromatic region (bottom)

Figure 12. Collision induced dissociation (CID) mass spectra of m/z 221 from: (a) human serum subject #2 (1, 4, 8, 12, 24 HPD) (b) synthetic standard (c) HPLC purified fraction from human liver S9 incubation with CP-122,721.

Downloaded from dmd.aspetjournals.org at ASPET Journals on June 24, 2024

DMD Fast Forward. Published on March 14, 2007 as DOI: 10.1124/dmd.106.014266
This article has not been copyedited and formatted. The final version may differ from this version.

Figure 13. Collision induced dissociation (CID) mass spectra of m/z 409 for M16 from Human Urine (subject #2).

Figure 14. Collision induced dissociation (CID) mass spectra of m/z 384 for M17 from Human Urine (subject #2).

Figure 15. Collision induced dissociation (CID) mass spectra of m/z 402 for M18 from Human Urine (subject #5).

Figure 16. Proposed Biotransformation Pathways of [^{14}C]-CP-122,721 in Humans

Figure 17. Proposed mechanisms for the formation of human serum metabolite M15 (TFMSA). TFMSA = 5-trifluoromethoxy salicylic acid)

Downloaded from dmd.aspetjournals.org at ASPET Journals on June 24, 2024

DMD Fast Forward. Published on March 14, 2007 as DOI: 10.1124/dmd.106.014266
This article has not been copyedited and formatted. The final version may differ from this version.

Table 1. Radiolabeled Mass Balance of CP-122,721 in Humans Administered a 30 mg (free base)/kg PO Dose

		Percentage of Total ^{14}C Excreted from 0 - 312 Hours Post Dose		
	Subject #	**Urine**	**Feces**	**Total**
Extensive Metabolizers (EM)	1	78.8	9.4	88.2
	2	85.2	2.3	87.5
	3	74.7	9.6	84.3
	4	84.0	4.9	88.9
	Mean	**80.7**	**6.6**	**87.2**
	SD	**4.9**	**3.6**	**2.0**
Poor Metabolizers (PM)	5	65.0	6.9	71.9
	6	77.2	6.9	84.1
	Mean	**71.1**	**6.9**	**78.0**

Downloaded from dmd.aspetjournals.org at ASPET Journals on June 24, 2024

DMD Fast Forward. Published on March 14, 2007 as DOI: 10.1124/dmd.106.014266
This article has not been copyedited and formatted. The final version may differ from this version.

Table 2. Comparison of Mean Values of $AUC_{0\text{-tlast}}$, $t_{1/2}$ and C_{max} for Total Radioactivity and CP-122,721 in Human Serum Following Oral Administration of [^{14}C]-CP-122,721.

		Extensive Metabolizers (mean ±SD, n=4)	**Poor Metabolizers (mean, n=2)**
$AUC_{0\text{-tlast}}$ (ng·hr/mL)	CP-122,721	64.6 ±23	3250
	Total Radioactivity	13600 ±3450	20300
	Drug % of Total Radioactivity	0.5	16
$t_{1/2}$ (hr)	CP-122,721	6.71 ±1	45
	Total Radioactivity	23.7 ±5	55.2
C_{max} (ng/mL) (ng(eq)/mL)	CP-122,721	7.4 ±3	69.8
	Total Radioactivity	844 ±152	447
	Drug % of Total Radioactivity	0.9	15.6

Downloaded from dmd.aspetjournals.org at ASPET Journals on June 24, 2024

DMD Fast Forward. Published on March 14, 2007 as DOI: 10.1124/dmd.106.014266
This article has not been copyedited and formatted. The final version may differ from this version.

Table 3. Average Percentages of Urinary and Fecal Metabolites of CP-122,721 in EM and PM Human Subjects Following Administration of a 30 mg (free dose) Oral Dose

Metabolite	m/z	Description	% Dose for EM # (mean ±SD, n=4) Urine	Feces	% Dose for PM # (mean, n=2) Urine	Feces
M16	409	Piperadine dione	2.3 ±0.3	ND	2.5	ND
M1	475	Hydroquinone + Gluc	4.1 ±5	ND	ND	ND
M17	384	Desmethyl + N-dealkyl + Gluc	4.5 ±1	ND	3.1	ND
M18	402	Desmethyl + Oxidative deamination + Gluc	10.9 ±2	ND	9.5	ND
M12	288	Desmethyl + N-dealkyl + Sulfation	2.9 ±1	ND	0.8	ND
M2	573	OH + Gluc	7.3 ±2	ND	2.7	ND
M3	559	Desmethyl + OH + Gluc	5.5 ±1	ND	6.8	ND
M14	559	Desmethyl + OH + Gluc	5.3 ±1	ND	10.7	ND
M19	557	Desmethyl + Lactam + Gluc	6.3 ±2	ND	17.2	ND
M4	543	Desmethyl + Gluc	27.5 ±9	ND	ND	ND
M20	573	Desmethyl + Lactam + OH+ Gluc	7.3 ±3	ND	2.7	ND
M15 (TFMSA)	221	Trifluoromethoxy Salicylic Acid	1.4 ±0.2	ND	3.5	ND
M7	383	Desmethyl + OH	ND	6.1 *	ND	ND
M8	367	Desmethyl	ND	3.4 *	ND	ND
CP-122,721	381	Parent	0.4 ±0.3	ND	1.9	4.63
M9	381	Desmethyl + Lactam	ND	ND	ND	2.27
Totals			95.2		68.4	

ND = Not Detected
EM = Extensive Metabolizers
PM = Poor Metabolizers
* detected in 2 subjects
# % dose is calculated based on total % ^{14}C excreted from urine and feces of each subject shown in Table 1
(% dose Mx = %radioactivity Mx * total % ^{14}C excreted)

Downloaded from dmd.aspetjournals.org at ASPET Journals on June 24, 2024

DMD Fast Forward. Published on March 14, 2007 as DOI: 10.1124/dmd.106.014266
This article has not been copyedited and formatted. The final version may differ from this version.

Table 4. Average Percentages of Serum Metabolites of [^{14}C] CP-122,721 in EM and PM Human Subjects After Administration of a 30 mg (free base) Oral Dose

Metabolite	% of Total Radioactivity in Human Serum (HPD)	
	EM Subjects (mean ±SD, n=4)	PM Subjects (mean, n=2)
M 3	25.2 ±7	62.3
M 4	13.6 ±3	N. D.
M5	5.2 ±1	2.1
M15 (TFMSA)	55.9 ±5	29.4
CP-122,721	N. D.	5.6
Total	**99.9**	**99.4**

N. D. = Not Detected
EM = Extensive Metabolizer
PM = Poor Metabolizer
TFMSA = 5-trifluoromethoxy salicylic acid

Downloaded from dmd.aspetjournals.org at ASPET Journals on June 24, 2024

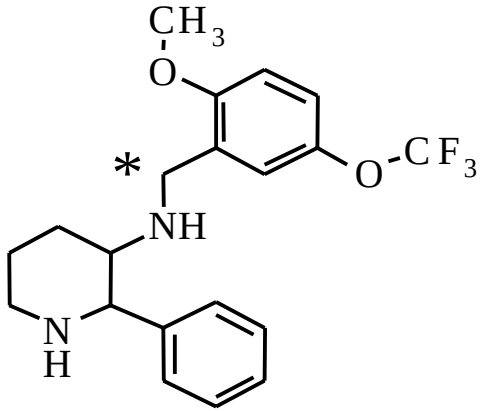

* ^{14}C label

Figure 1

DMD Fast Forward. Published on March 14, 2007 as DOI: 10.1124/dmd.106.014266
This article has not been copyedited and formatted. The final version may differ from this version.

Downloaded from dmd.aspetjournals.org at ASPET Journals on June 24, 2024

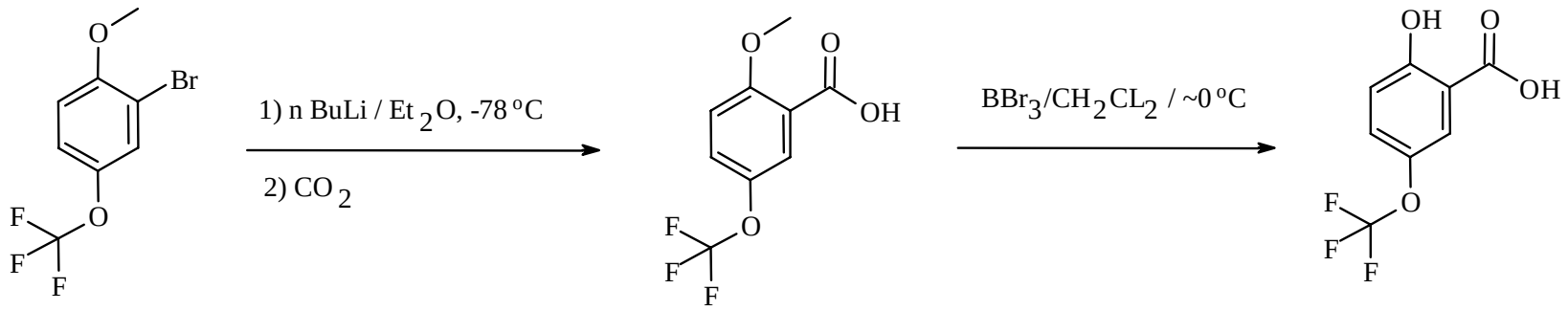

2-Bromo-1-methoxy-4 trifluoromethoxy-benzene

5-trifluoromethoxy salicylic acid (TFMSA)

Figure 2

DMD Fast Forward. Published on March 14, 2007 as DOI: 10.1124/dmd.106.014266
This article has not been copyedited and formatted. The final version may differ from this version.

Downloaded from dmd.aspetjournals.org at ASPET Journals on June 24, 2024

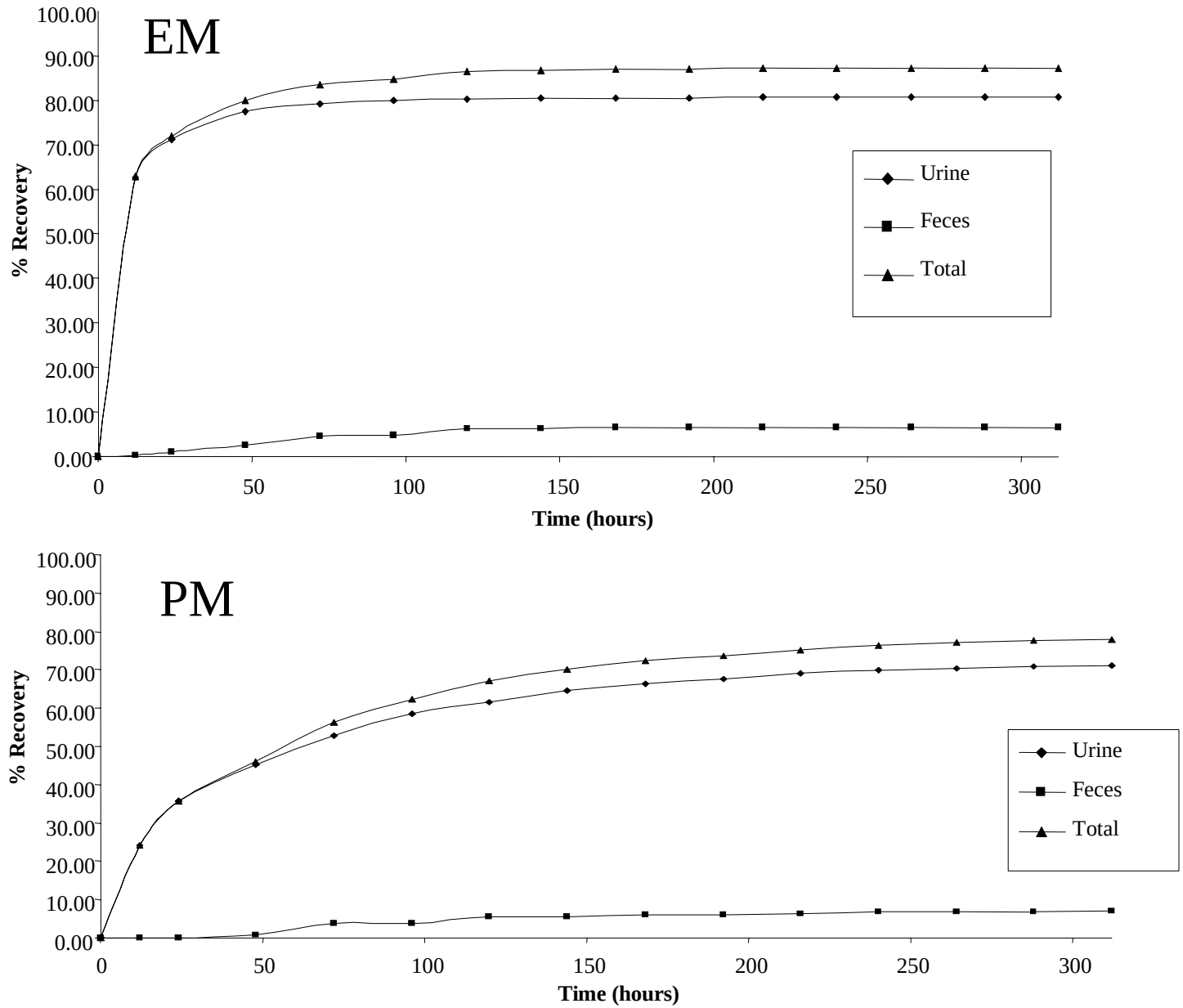

Figure 3

Downloaded from dmd.aspetjournals.org at ASPET Journals on June 24, 2024

DMD Fast Forward. Published on March 14, 2007 as DOI: 10.1124/dmd.106.014266
This article has not been copyedited and formatted. The final version may differ from this version.

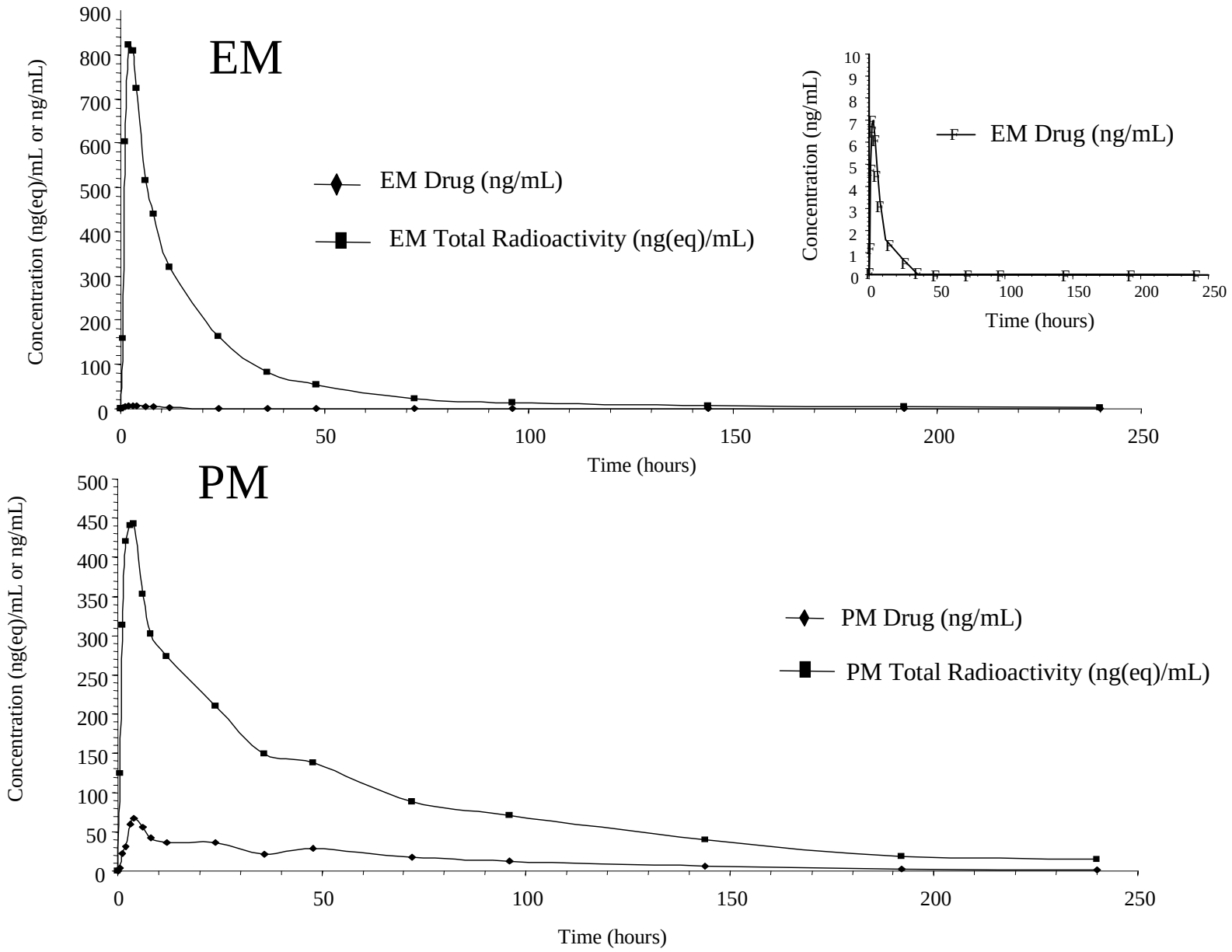

Figure 4

DMD Fast Forward. Published on March 14, 2007 as DOI: 10.1124/dmd.106.014266
This article has not been copyedited and formatted. The final version may differ from this version.

Downloaded from dmd.aspetjournals.org at ASPET Journals on June 24, 2024

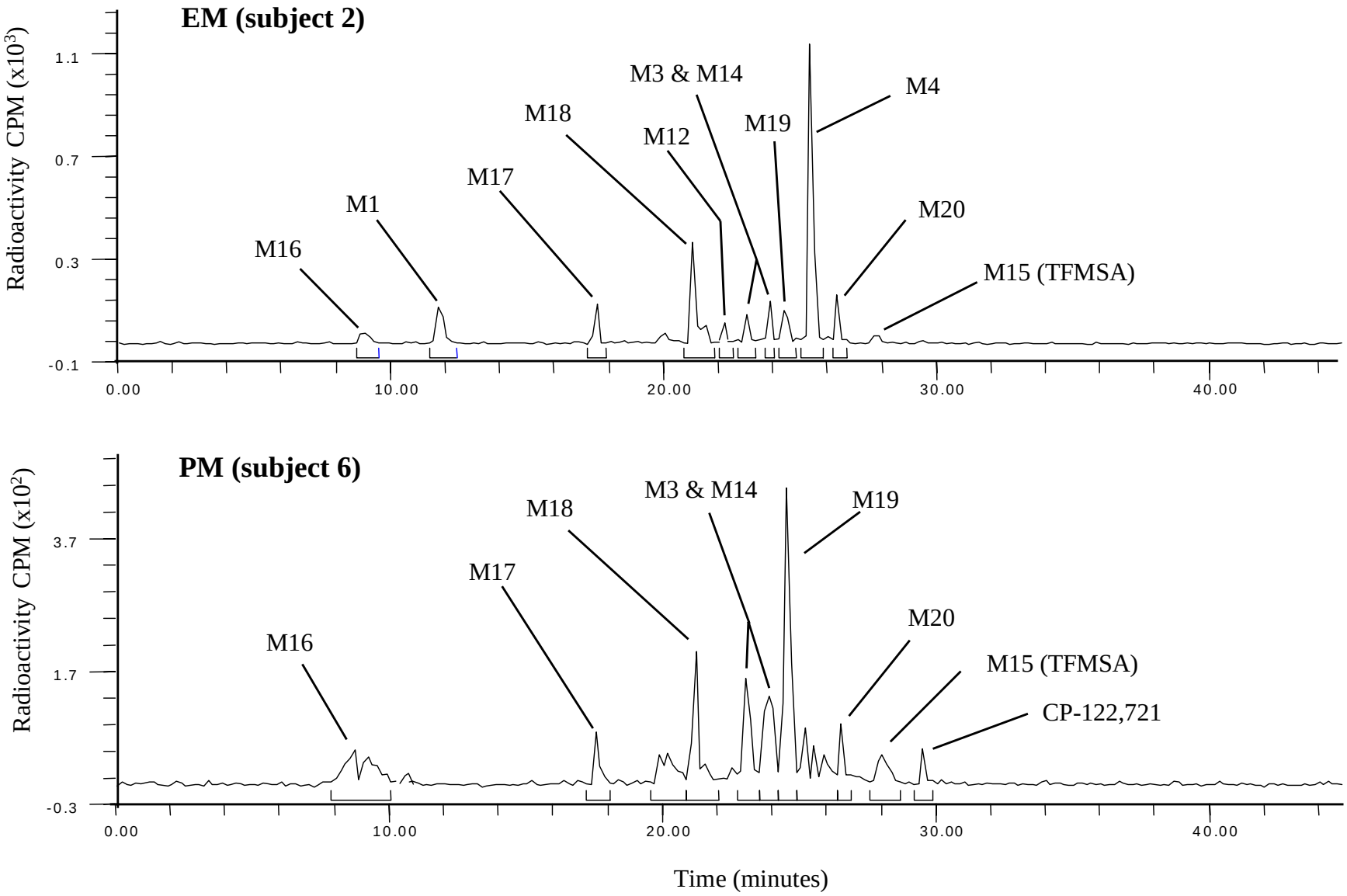

Figure 5

Downloaded from dmd.aspetjournals.org at ASPET Journals on June 24, 2024

DMD Fast Forward. Published on March 14, 2007 as DOI: 10.1124/dmd.106.014266
This article has not been copyedited and formatted. The final version may differ from this version.

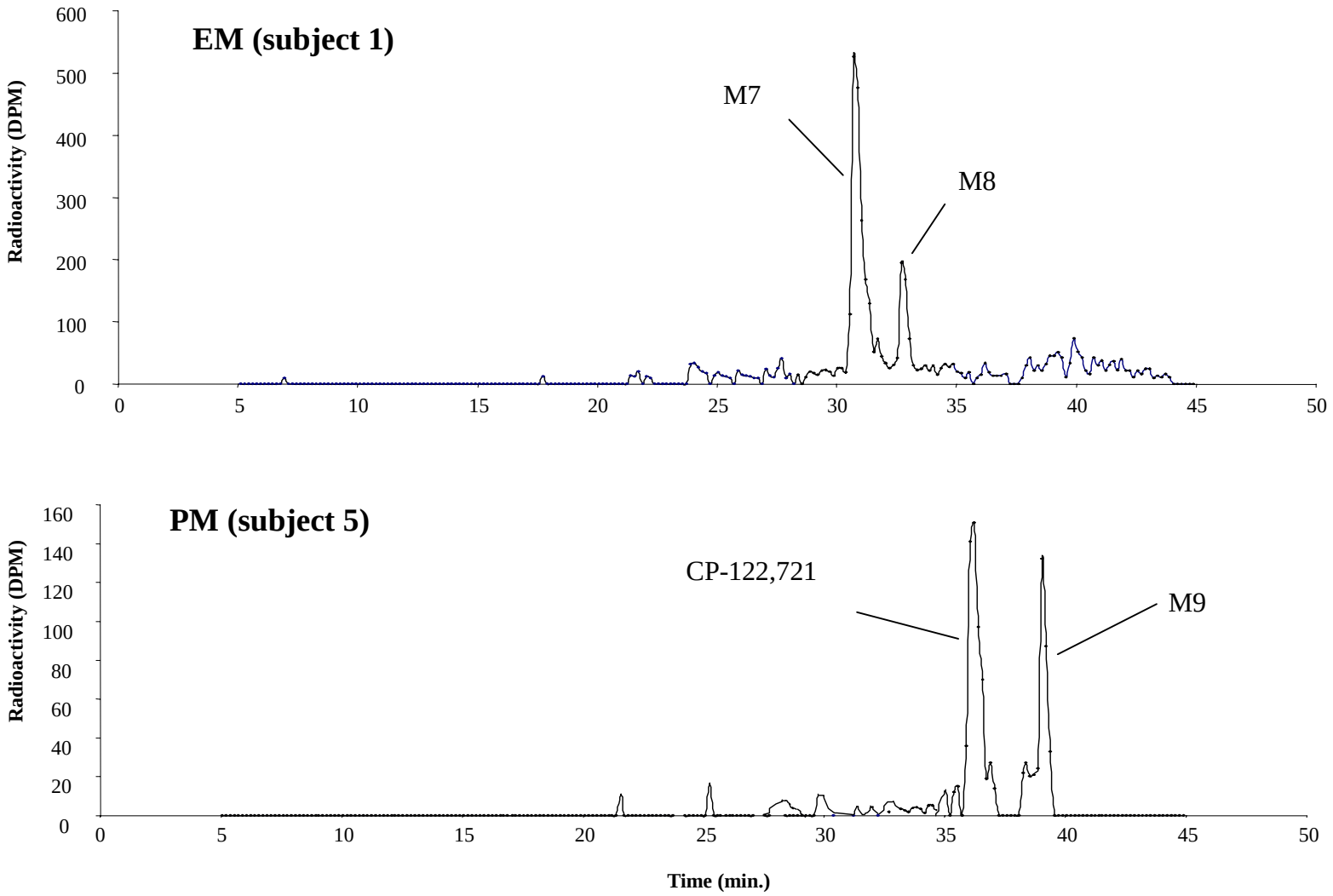

Figure 6

Downloaded from dmd.aspetjournals.org at ASPET Journals on June 24, 2024

DMD Fast Forward. Published on March 14, 2007 as DOI: 10.1124/dmd.106.014266
This article has not been copyedited and formatted. The final version may differ from this version.

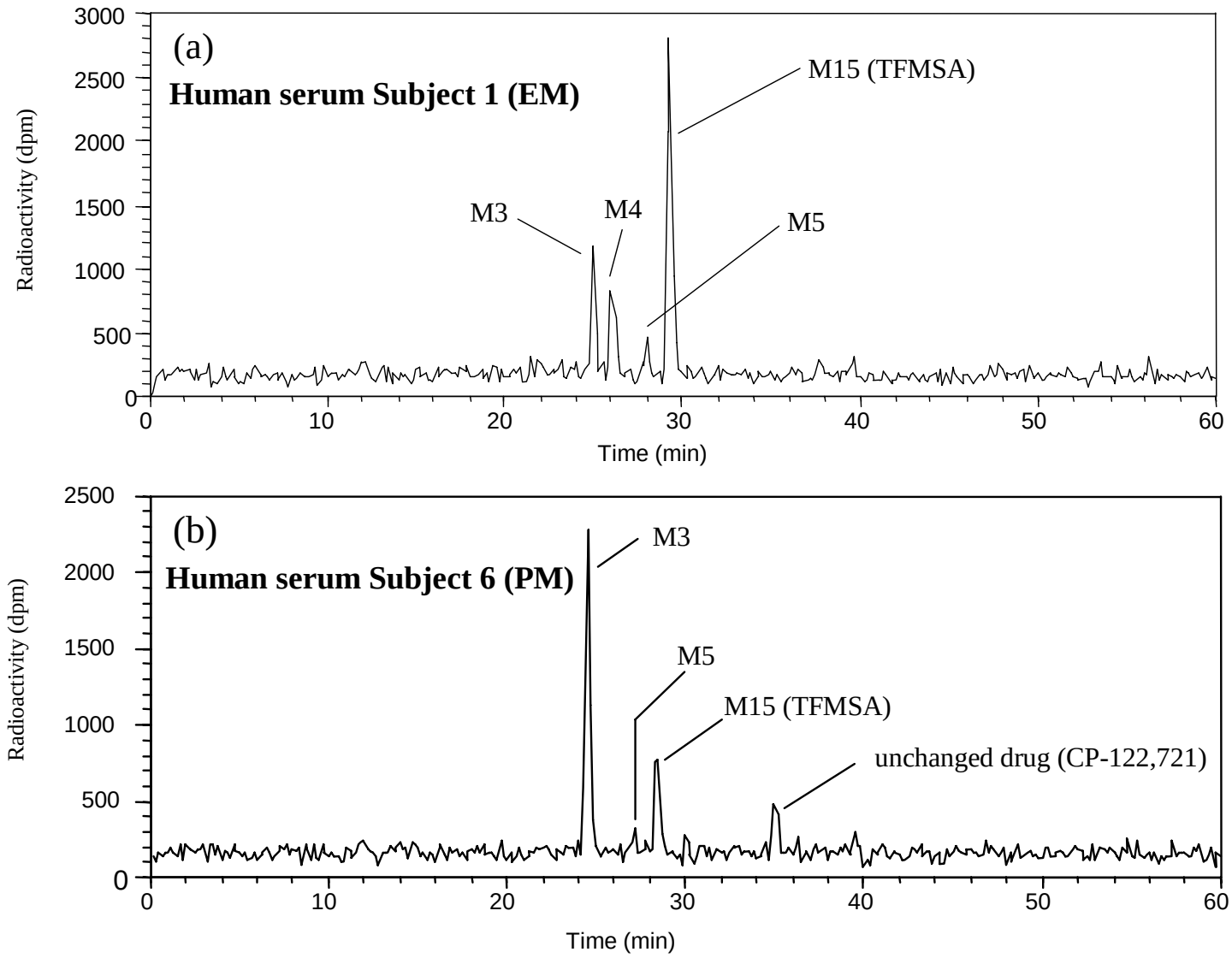

Figure 7

DMD Fast Forward. Published on March 14, 2007 as DOI: 10.1124/dmd.106.014266
This article has not been copyedited and formatted. The final version may differ from this version.

Downloaded from dmd.aspetjournals.org at ASPET Journals on June 24, 2024

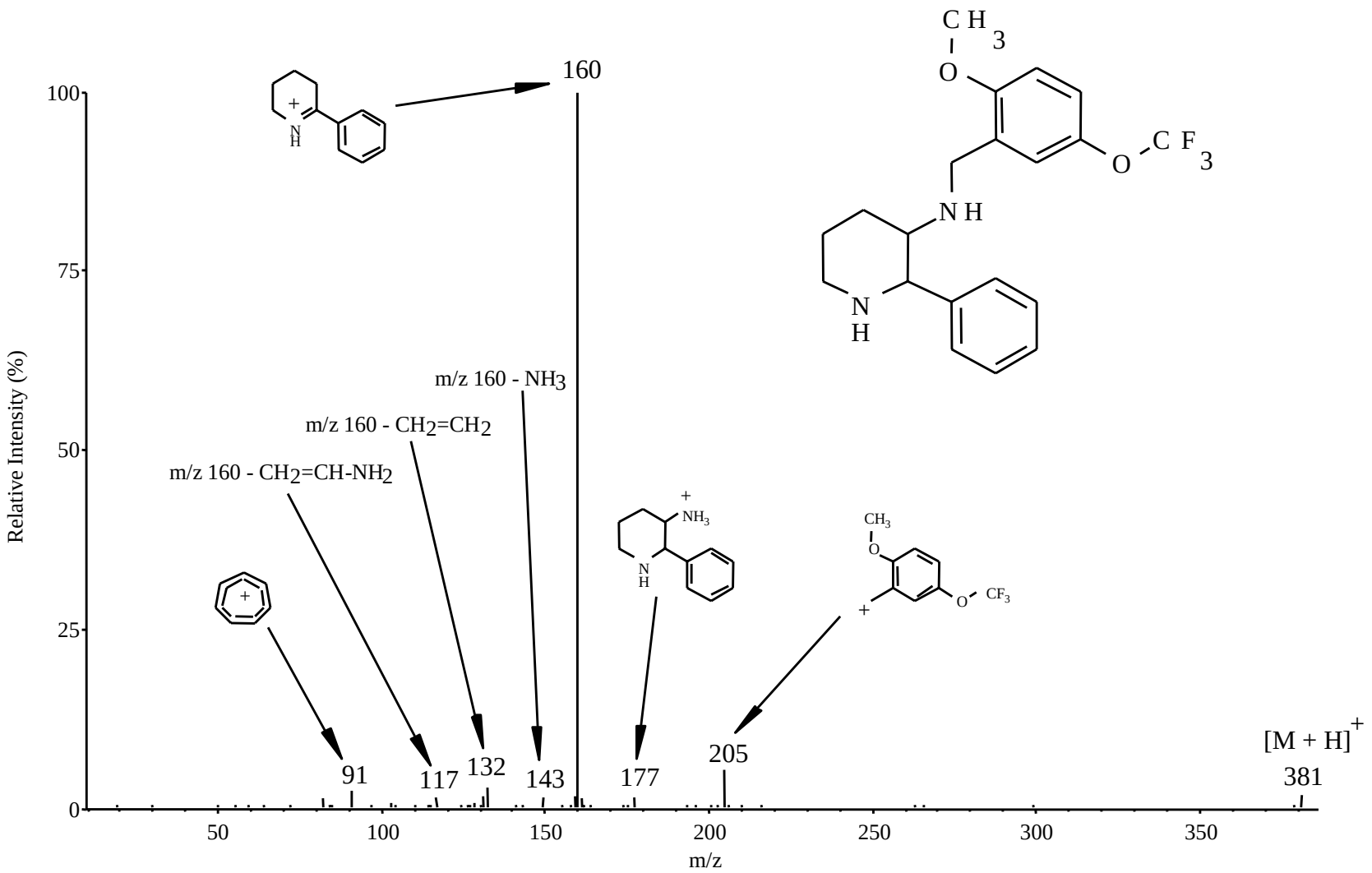

Figure 8

Downloaded from dmd.aspetjournals.org at ASPET Journals on June 24, 2024

DMD Fast Forward. Published on March 14, 2007 as DOI: 10.1124/dmd.106.014266
This article has not been copyedited and formatted. The final version may differ from this version.

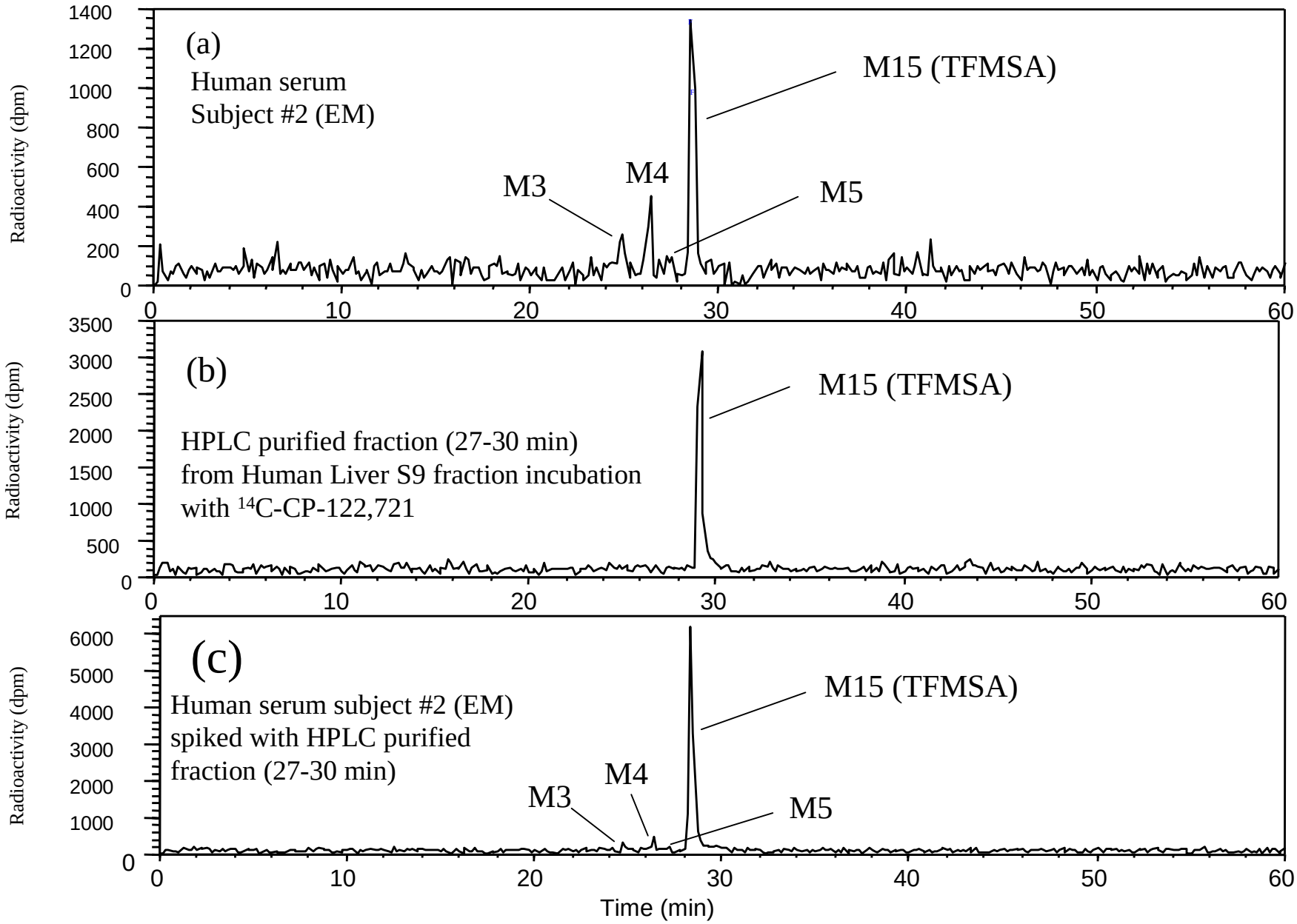

Figure 9

Downloaded from dmd.aspetjournals.org at ASPET Journals on June 24, 2024

DMD Fast Forward. Published on March 14, 2007 as DOI: 10.1124/dmd.106.014266
This article has not been copyedited and formatted. The final version may differ from this version.

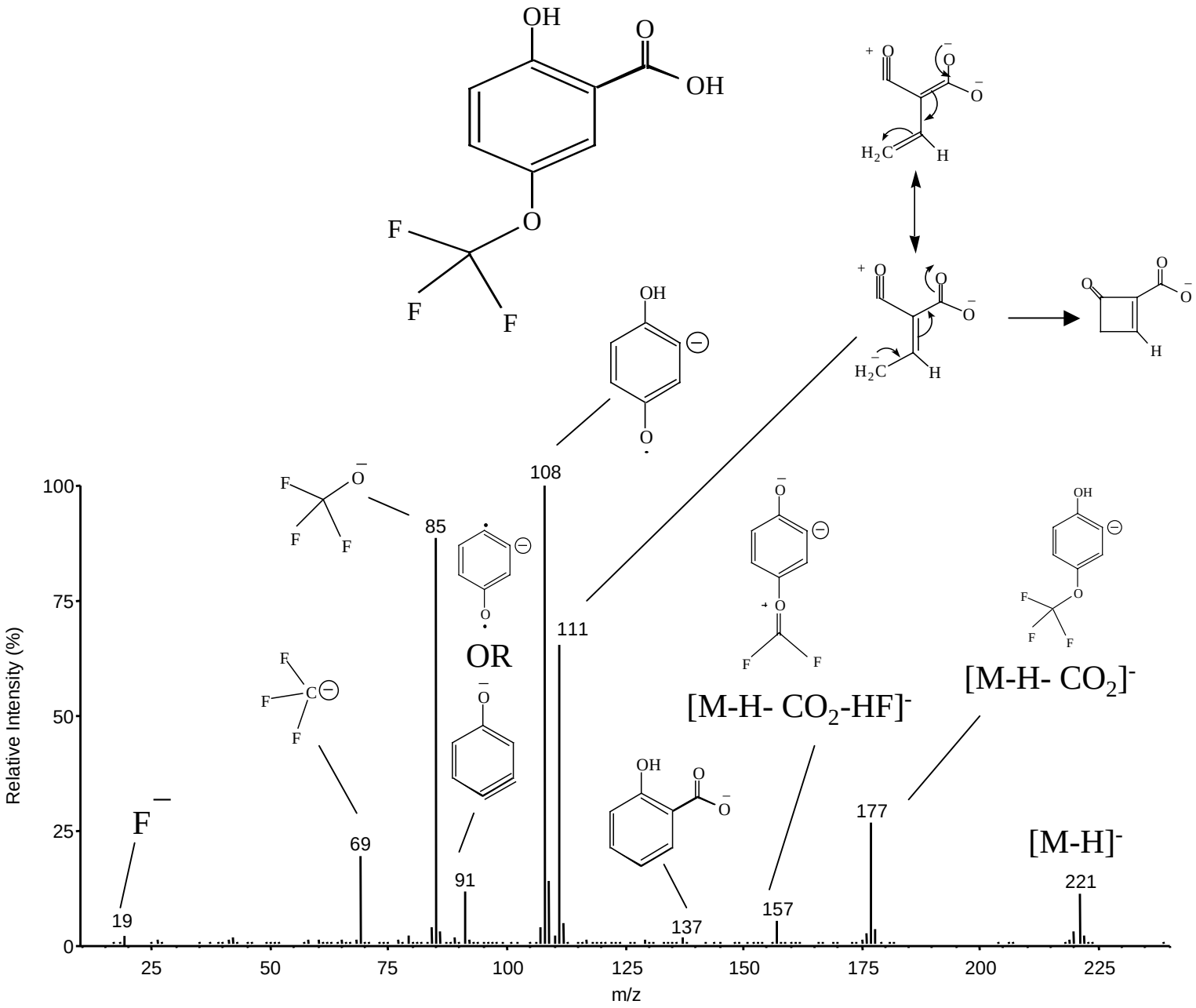

Figure 10

Downloaded from dmd.aspetjournals.org at ASPET Journals on June 24, 2024

DMD Fast Forward. Published on March 14, 2007 as DOI: 10.1124/dmd.106.014266
This article has not been copyedited and formatted. The final version may differ from this version.

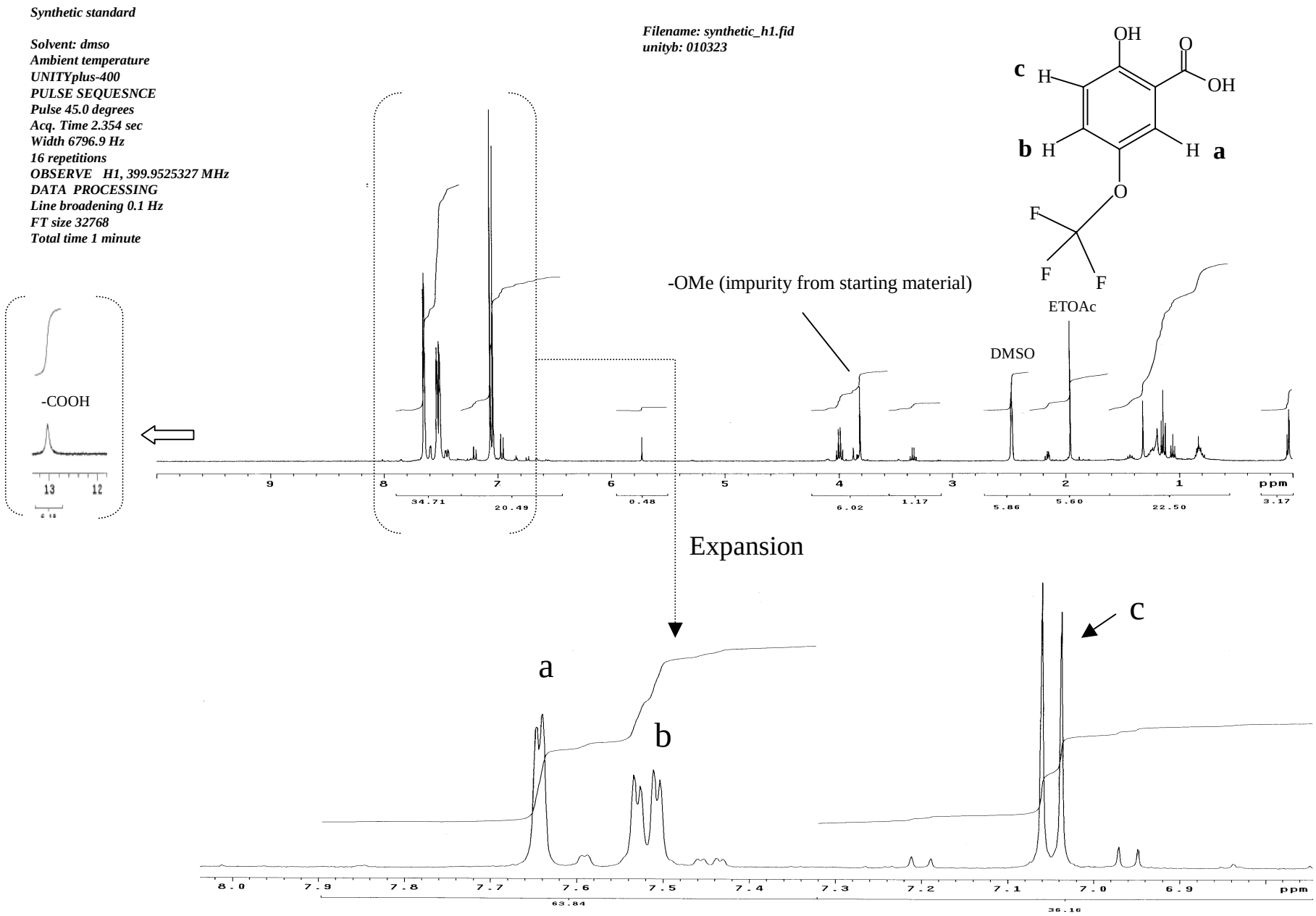

Figure 11

Downloaded from dmd.aspetjournals.org at ASPET Journals on June 24, 2024

DMD Fast Forward. Published on March 14, 2007 as DOI: 10.1124/dmd.106.014266
This article has not been copyedited and formatted. The final version may differ from this version.

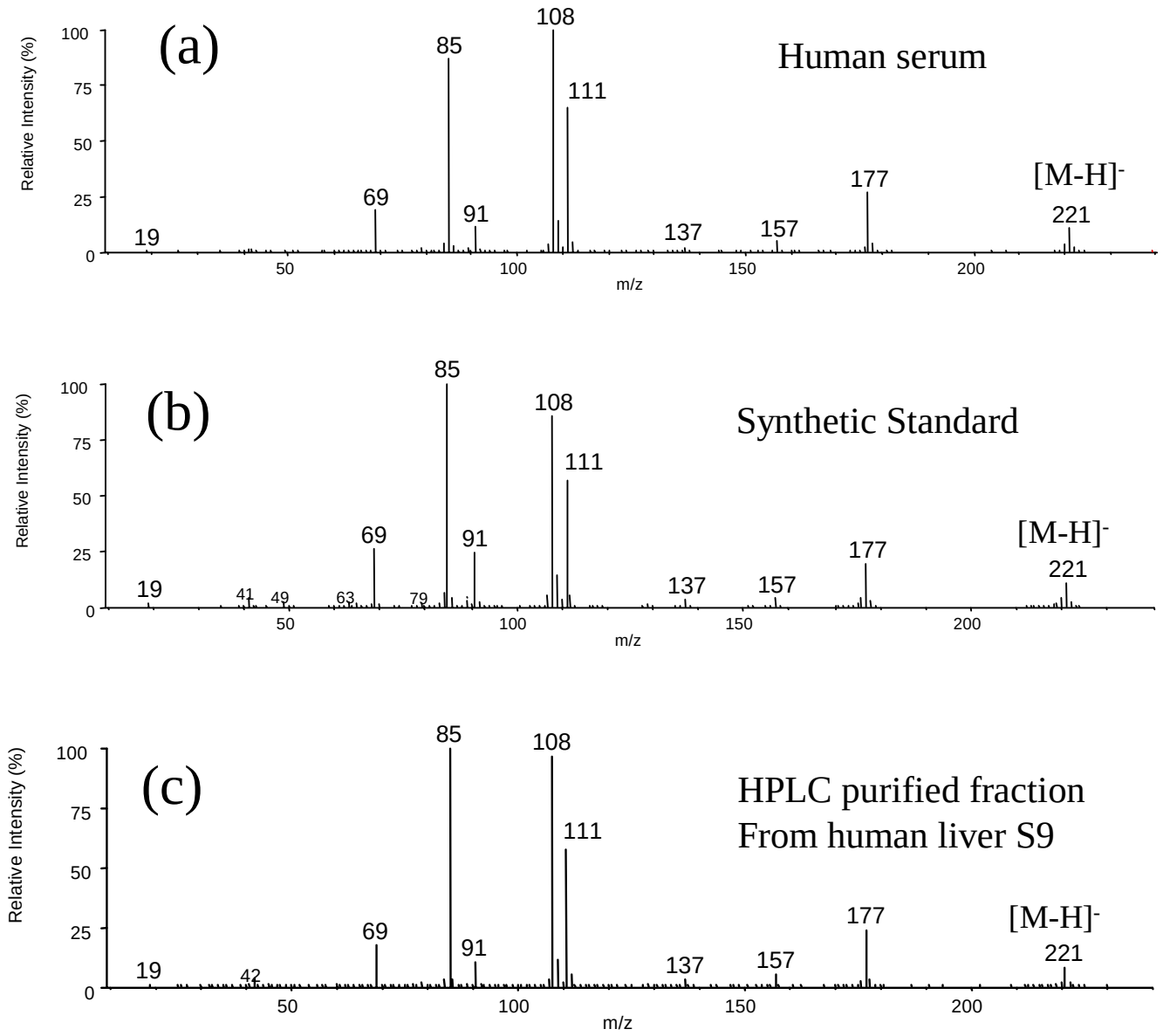

Figure 12

Downloaded from dmd.aspetjournals.org at ASPET Journals on June 24, 2024

DMD Fast Forward. Published on March 14, 2007 as DOI: 10.1124/dmd.106.014266
This article has not been copyedited and formatted. The final version may differ from this version.

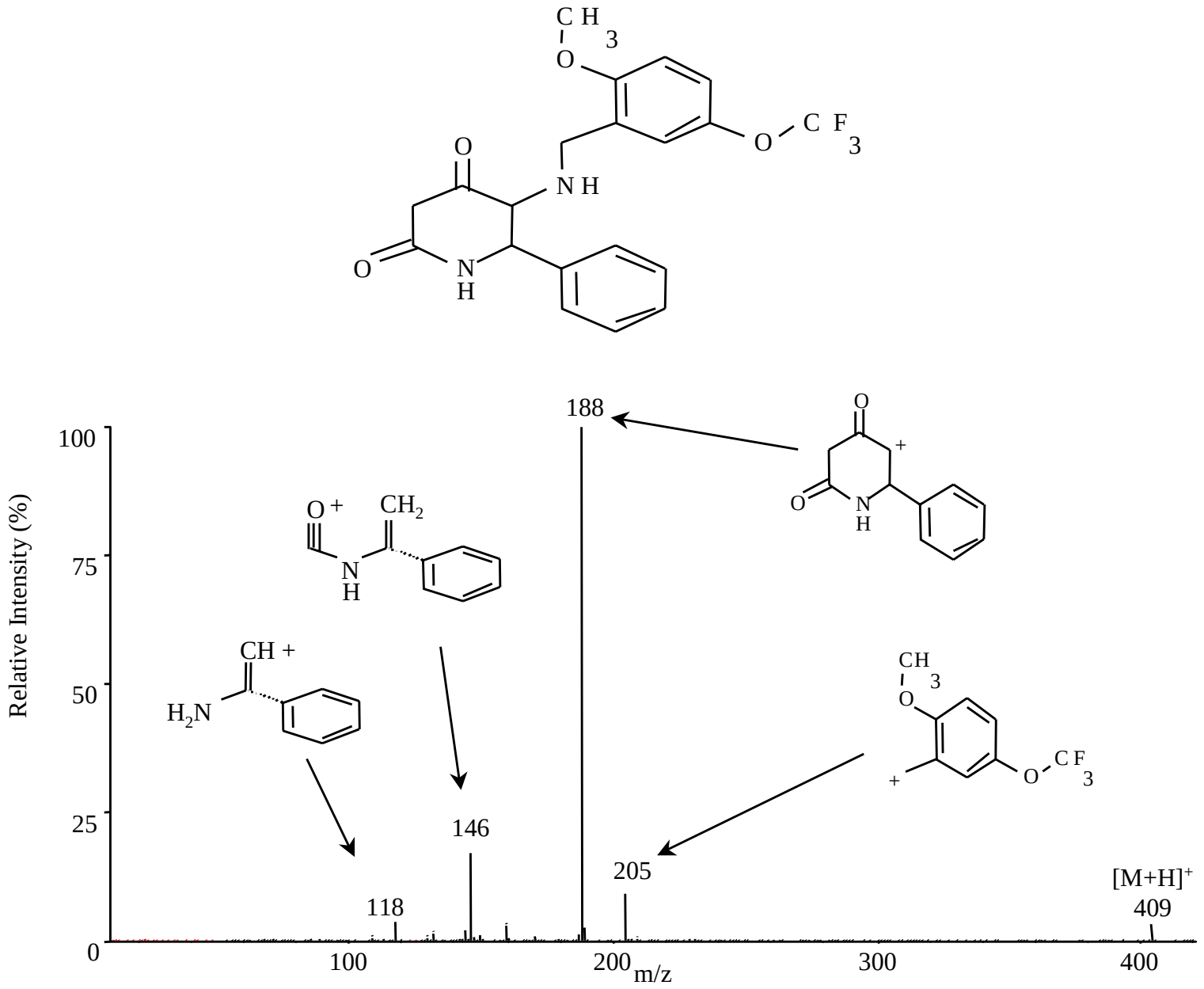

Figure 13

Downloaded from dmd.aspetjournals.org at ASPET Journals on June 24, 2024

DMD Fast Forward. Published on March 14, 2007 as DOI: 10.1124/dmd.106.014266
This article has not been copyedited and formatted. The final version may differ from this version.

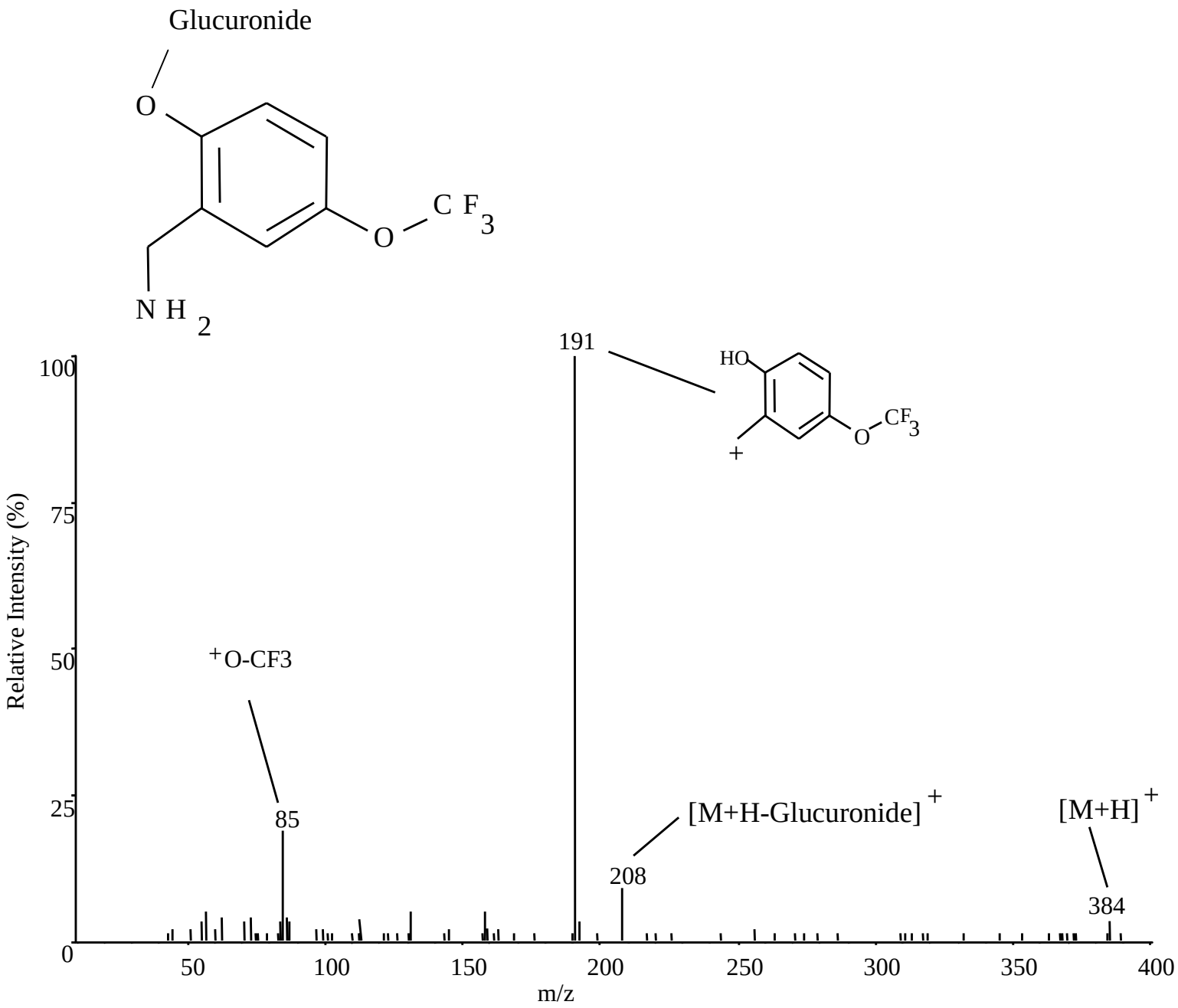

Figure 14

DMD Fast Forward. Published on March 14, 2007 as DOI: 10.1124/dmd.106.014266
This article has not been copyedited and formatted. The final version may differ from this version.

Downloaded from dmd.aspetjournals.org at ASPET Journals on June 24, 2024

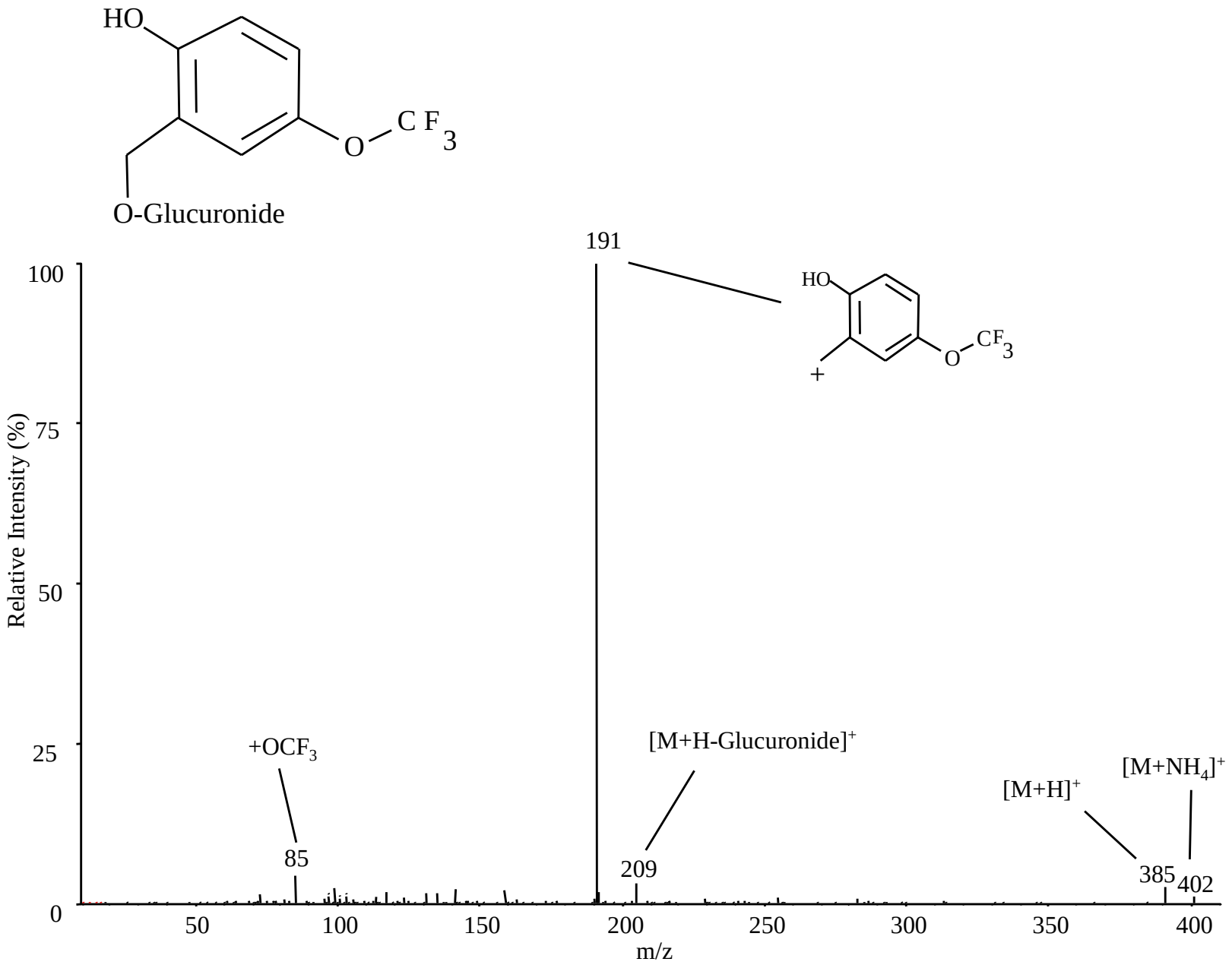

Figure 15

DMD Fast Forward. Published on March 14, 2007 as DOI: 10.1124/dmd.106.014266
This article has not been copyedited and formatted. The final version may differ from this version.

Downloaded from dmd.aspetjournals.org at ASPET Journals on June 24, 2024

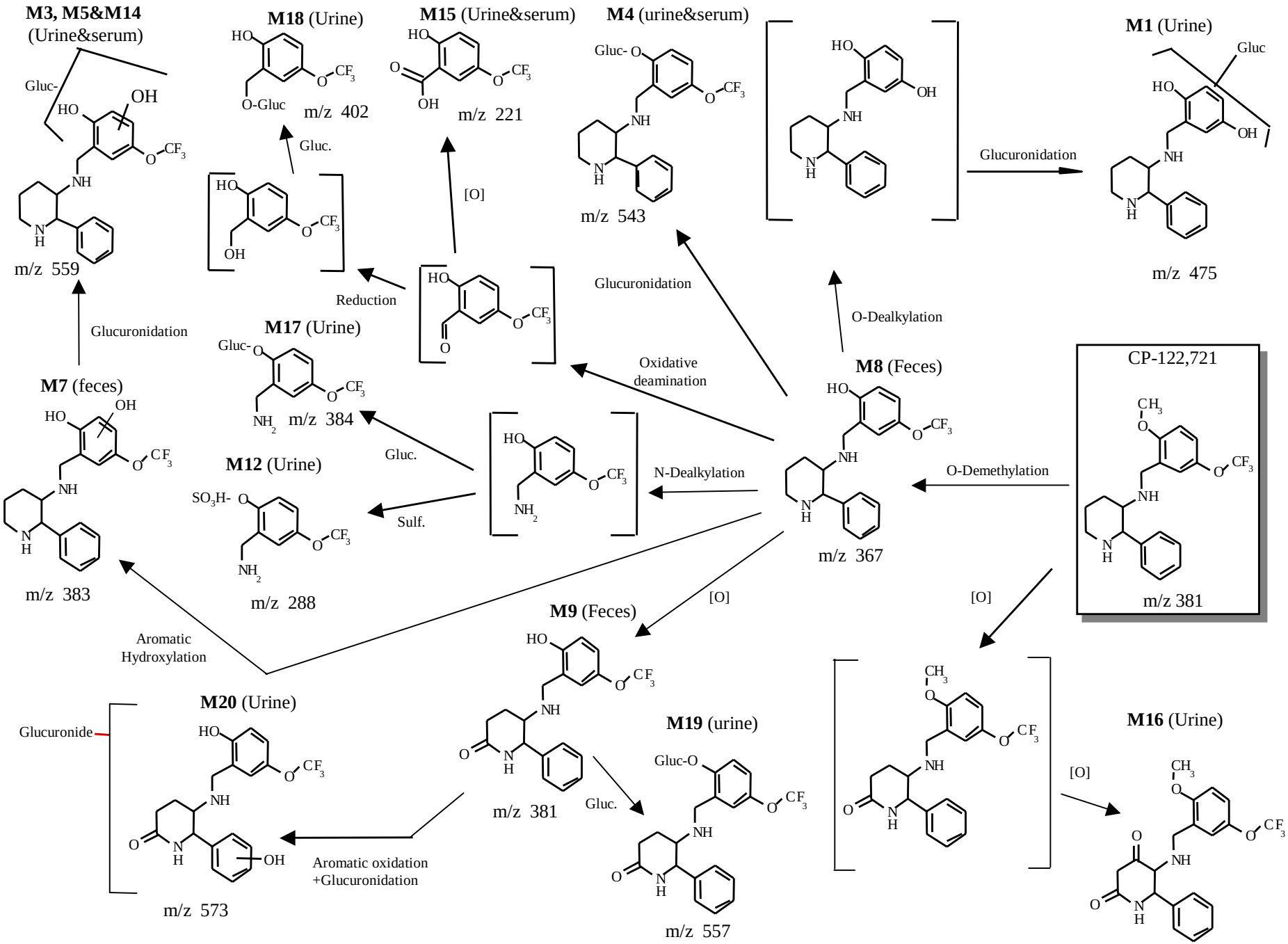

Figure 16

Downloaded from dmd.aspetjournals.org at ASPET Journals on June 24, 2024

DMD Fast Forward. Published on March 14, 2007 as DOI: 10.1124/dmd.106.014266
This article has not been copyedited and formatted. The final version may differ from this version.

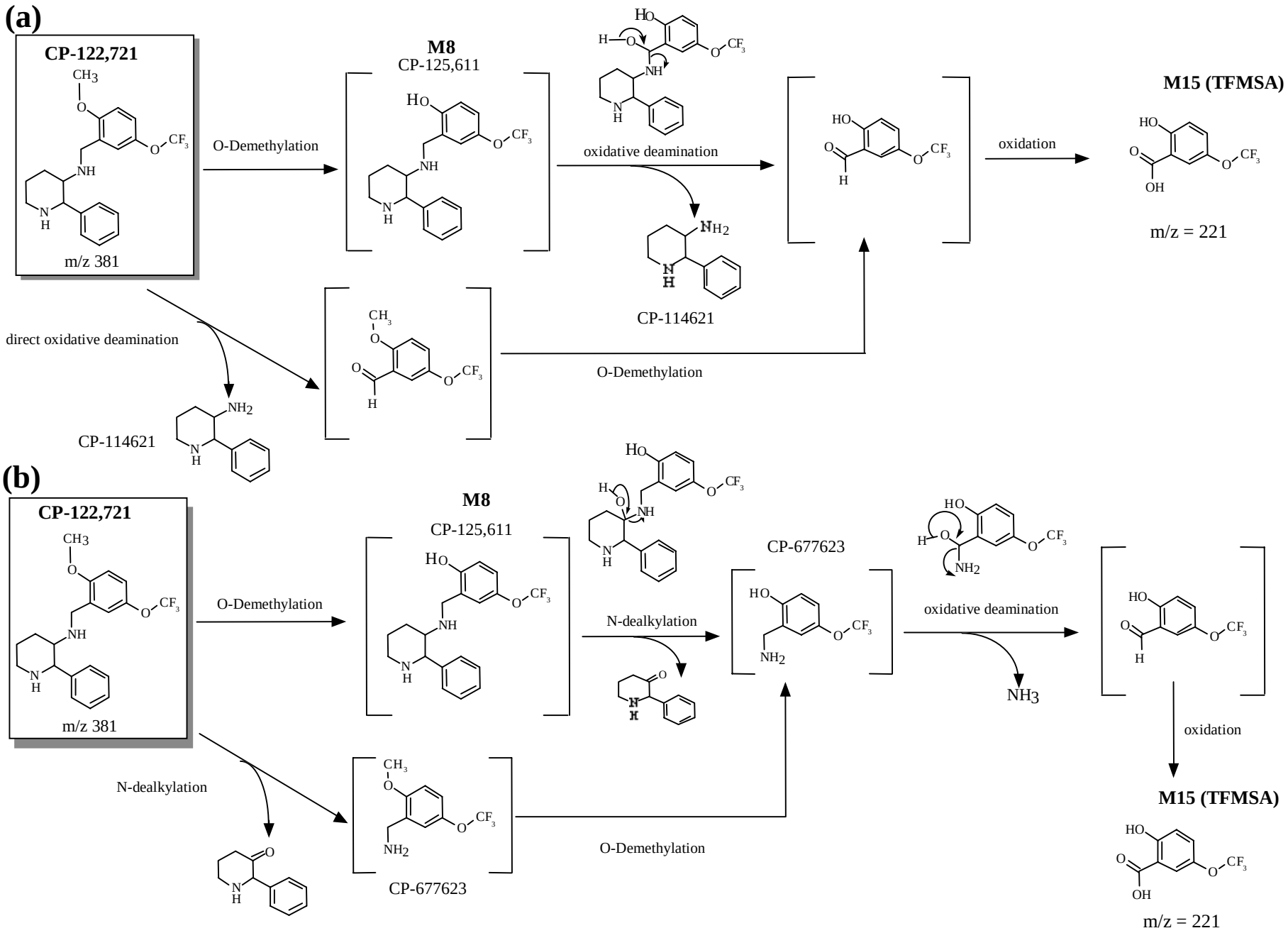

Figure 17

DMD Fast Forward. Published on March 14, 2007 as DOI: 10.1124/dmd.106.014266
This article has not been copyedited and formatted. The final version may differ from this version.

Downloaded from dmd.aspetjournals.org at ASPET Journals on June 24, 2024